Analytical theory of self-consistent current sheets in multicomponent relativistic plasma with arbitrary energy distribution of particles

Vl.V.Kocharovsky[1], V.V.Kocharovsky[1,2], V.Ju.Martyanov[1], S.V.Tarasov[1]

[1]*Institute of Applied Physics RAS, Nizhny Novgorod, Russia*
[2]*Texas A&M University, College Station, USA*

Analytical description of a new broad class of the neutral current configurations in a collisionless multicomponent plasma allows for functional freedom to the particle distribution functions and gives various spatial profiles of the self-consistent magnetic field and current.

Recent progress in analytic understanding of the self-consistent quasi-static configurations of magnetic field and current in an anisotropic collisionless multicomponent relativistic plasma with arbitrary energy distribution of particles is reviewed.

In typical planar and cylindrical geometries, we obtain a wide class of nonlinear stationary current structures which can be equally easily realized in relativistic and non-relativistic plasmas.

The solutions found are based on the method of integrals of motion, and extend far beyond the known generalizations of non-relativistic Harris and Bennett models. We come to the Grad-Shafranov type equation which allows us to analytically investigate and compare general properties of these structures. Namely, we discuss the ratio of magnetic field energy to that of particles, the anisotropy of particle momentum distribution, the spatial scales and profiles of particle density, current and magnetic field, etc.

Current sheet in Earth's magnetosphere

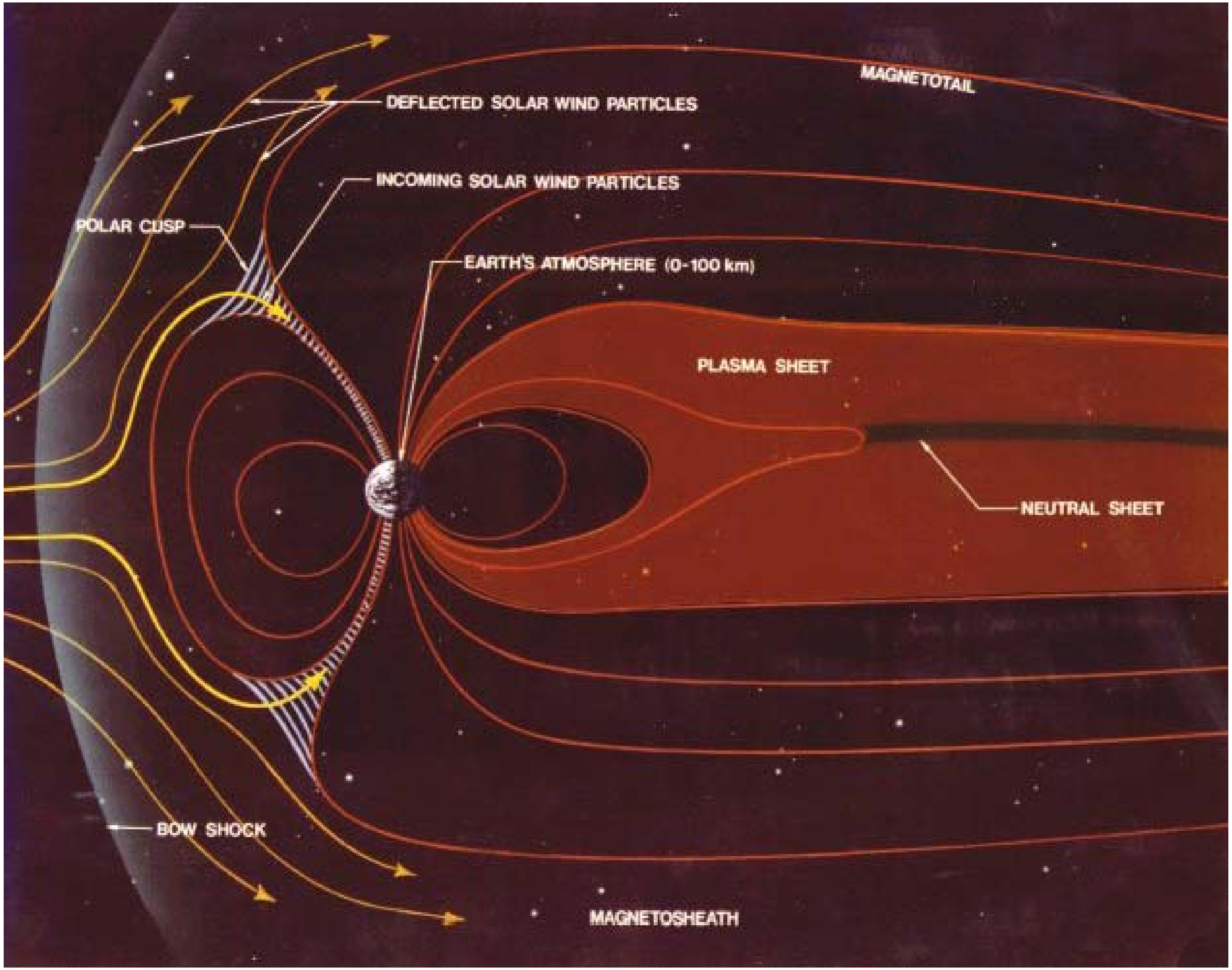

Cluster data show complicated structure of the current sheet

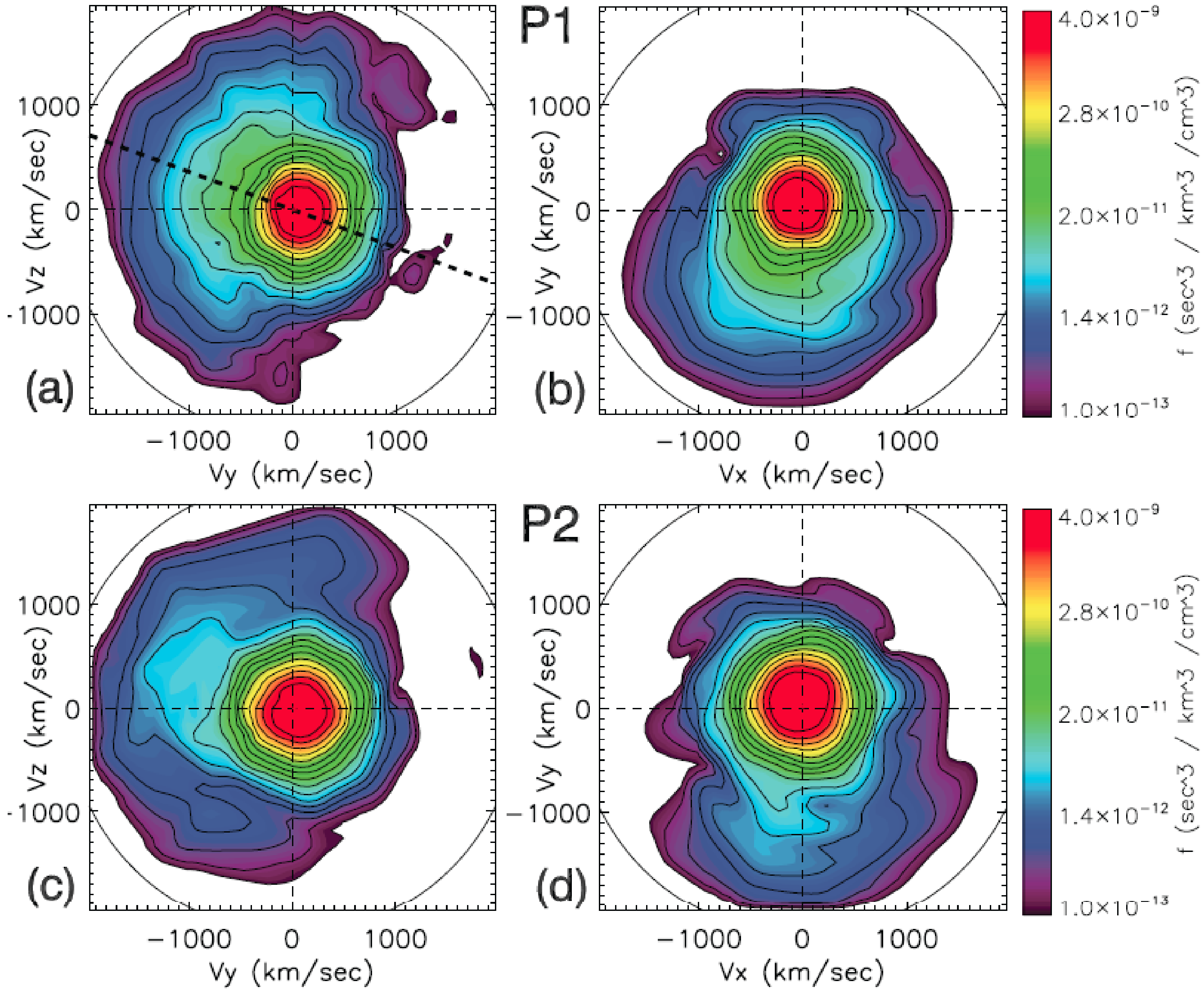

THEMIS P1 and P2 observations of the ion distribution functions in the despun spacecraft coordinates (+x is Earthward, +y is dawnward, and +z is southward) during the substorm event of 26 February 2008

Multi-scale and asymmetric current sheets in the Earth magnetosphere

Runov et al., Annales Geophysicae, ***24***, *247, 2006; Artemyev et al., Annales Geophysicae*, ***26***, *2749, 2008; Zelenyi et al., Plasma Physics Reports*, ***37***, *118, 2011.*

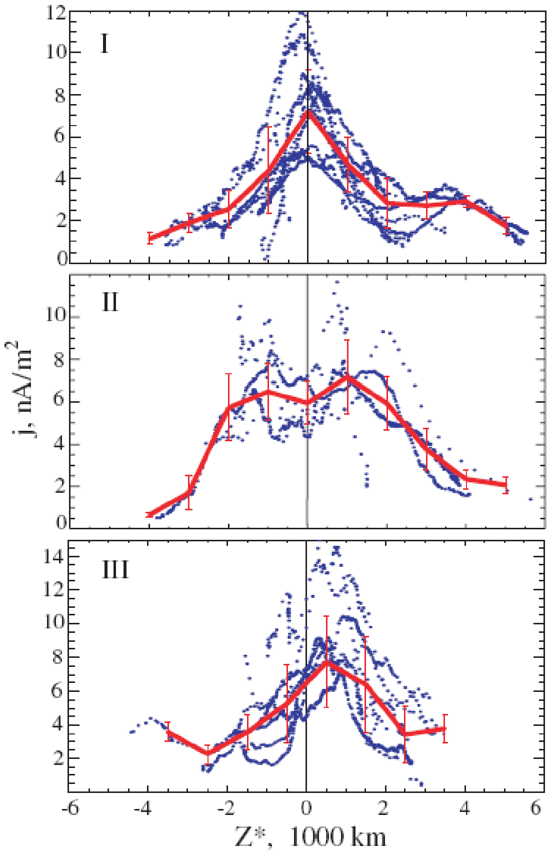

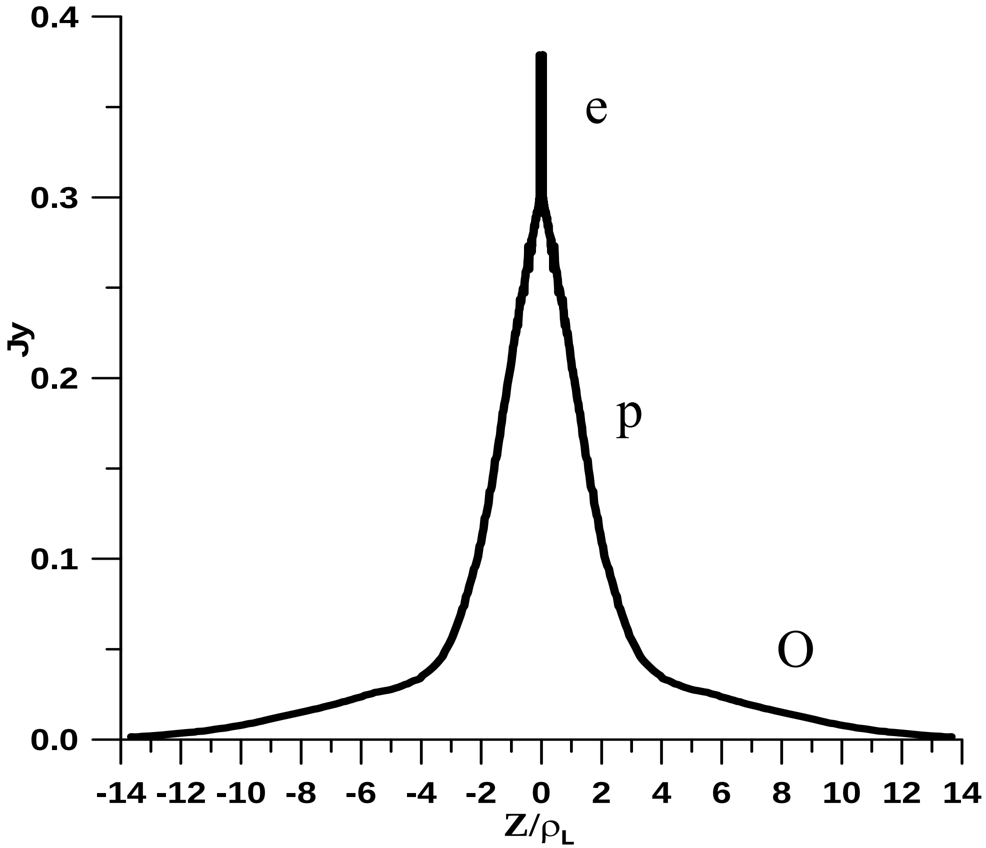

Nonlinear quasi-adiabatic current sheet model

Current sheet is formed due to the interaction of <u>ANISOTROPIC</u> plasma streams from northern/southern plasma mantles

Zelenyi et al. FNP'2013

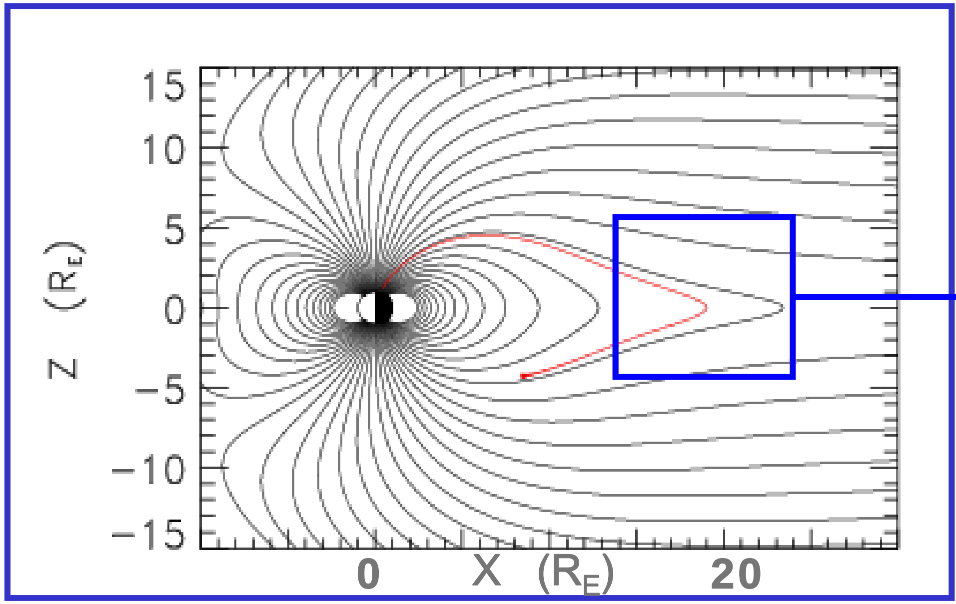

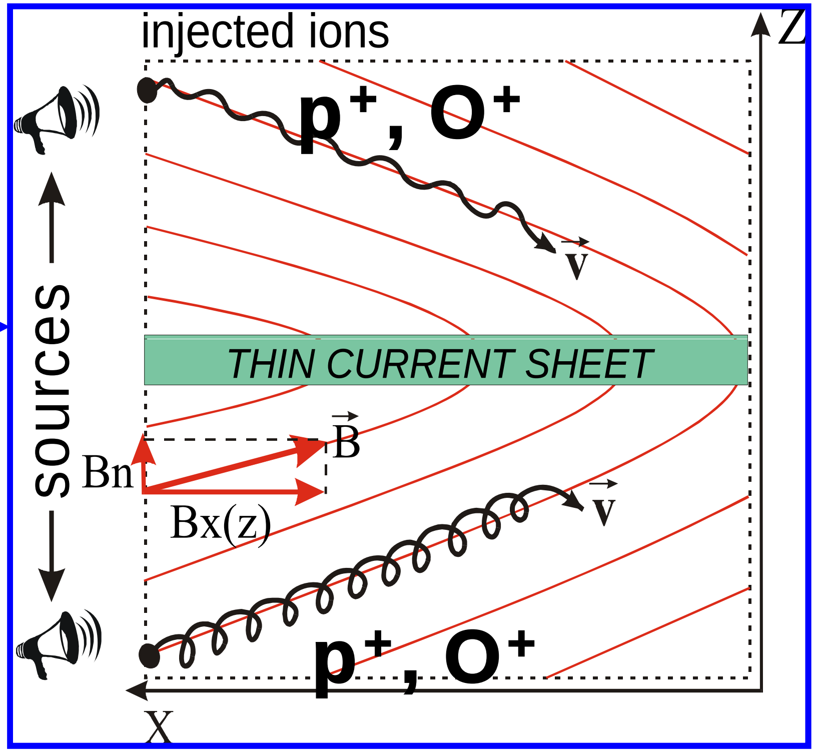

Adiabatic invariant $I_z = \dfrac{1}{2\pi}\oint p_z dz \approx \text{const}$

$$\kappa = \sqrt{\frac{R_{\min}}{\rho_{\max}}} \ll 1 \qquad R_{\min} = \frac{b_n}{db/dz}\bigg|_{z=0}$$

parameter of quasi-adiabaticity

H^+, O^+ ion dynamics is quasi-adiabatic

Electrons e^- are magnetized

Current sheets
and filaments
in solar corona:

Non-equilibrium
particle
distributions and
variety of spatial
profiles

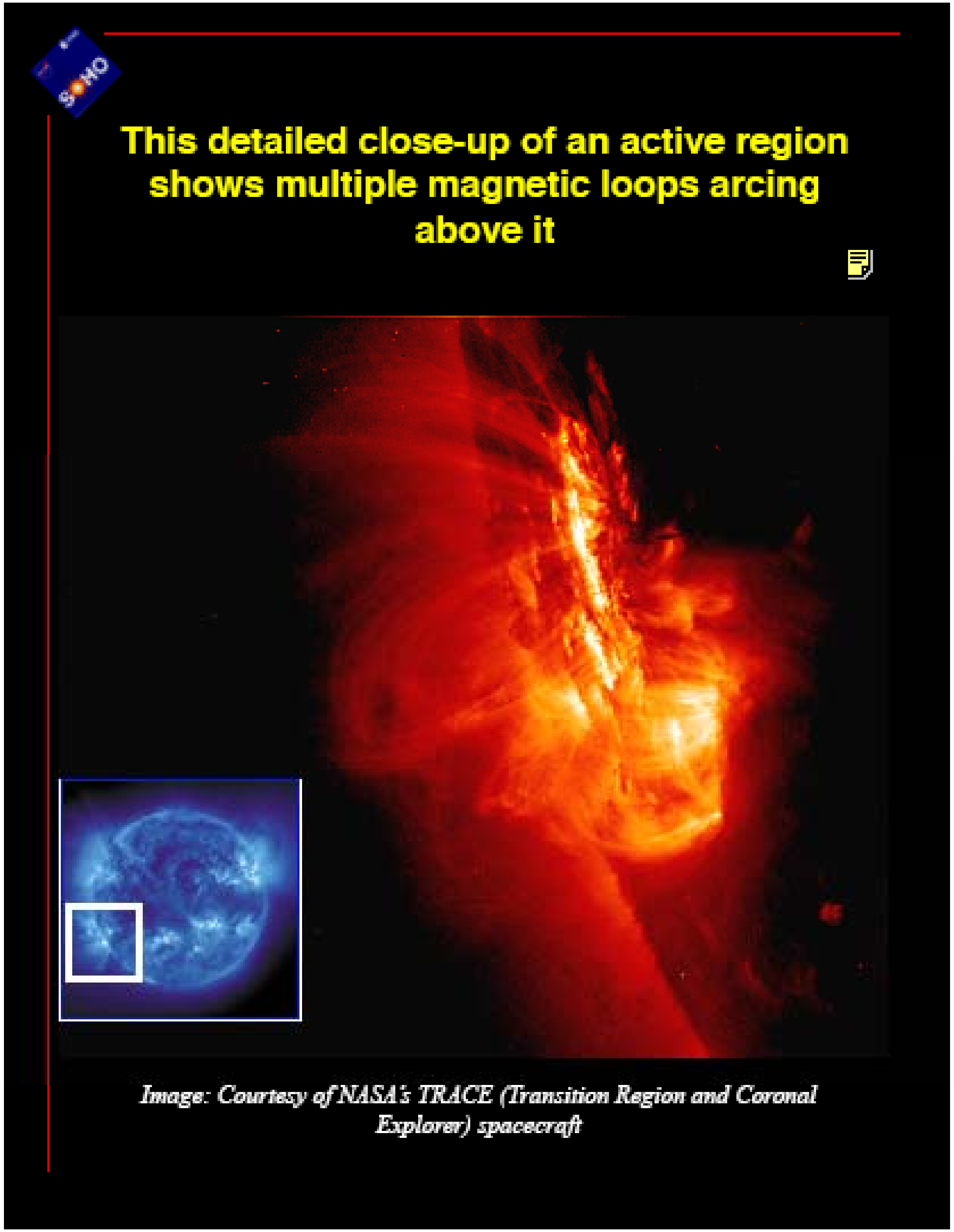

Relativistic collisionless current structures in systems with accretion

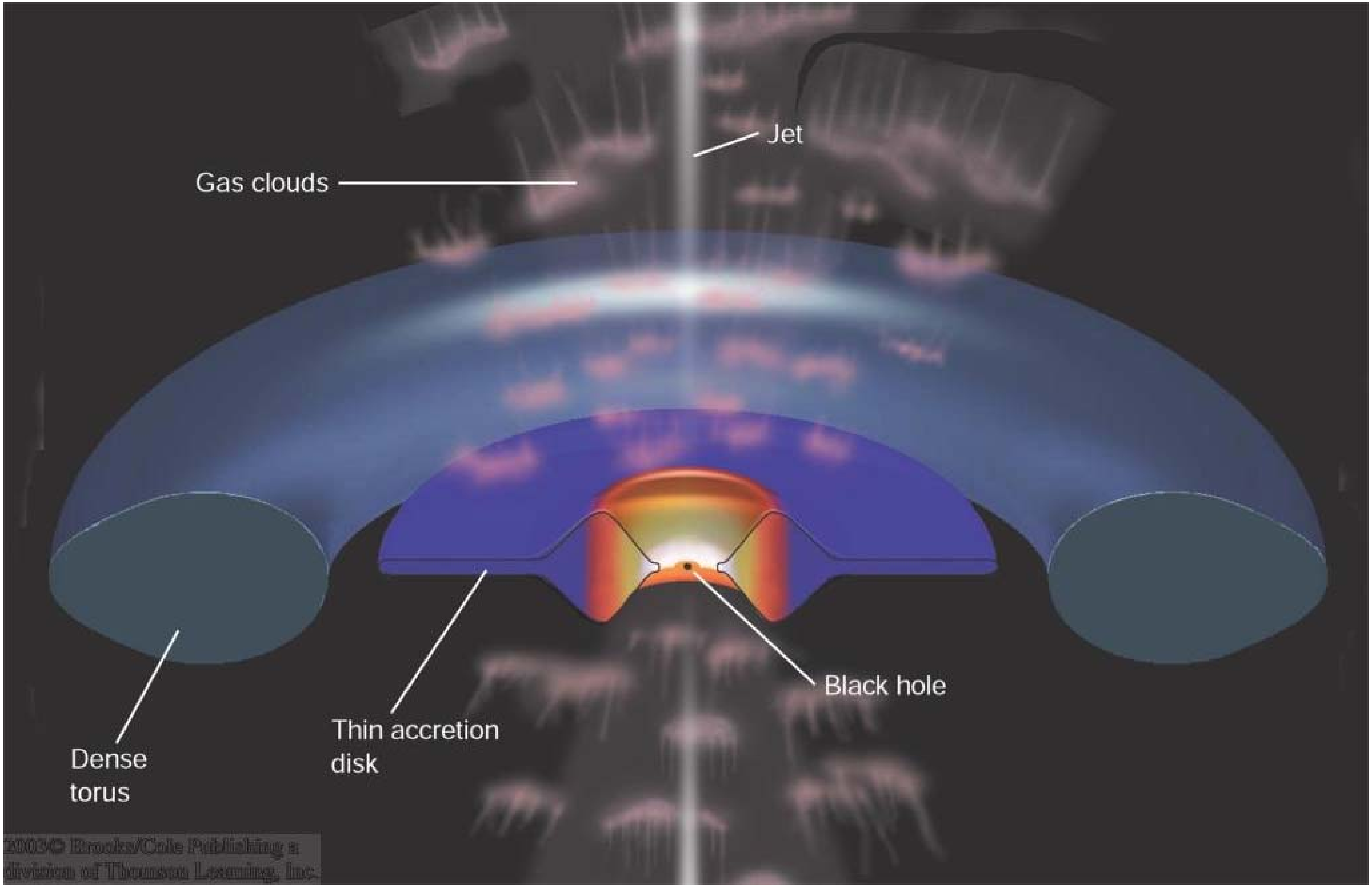

Relativistic shock model of Gamma-Ray Bursts (extremely non-equilibrium collisionless plasma with long-living turbulent magnetic field)

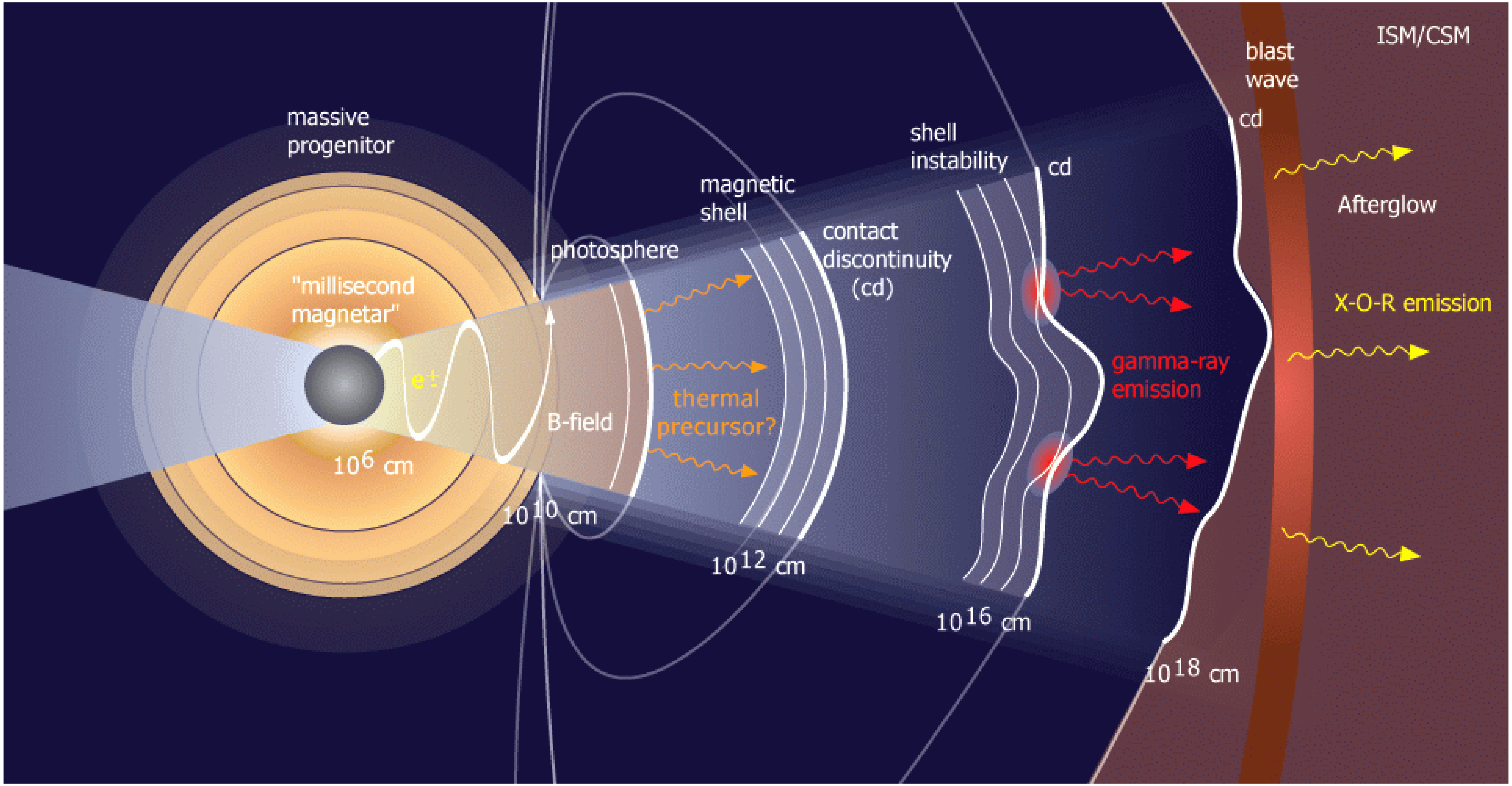

Current sheets in a pulsar wind nebula

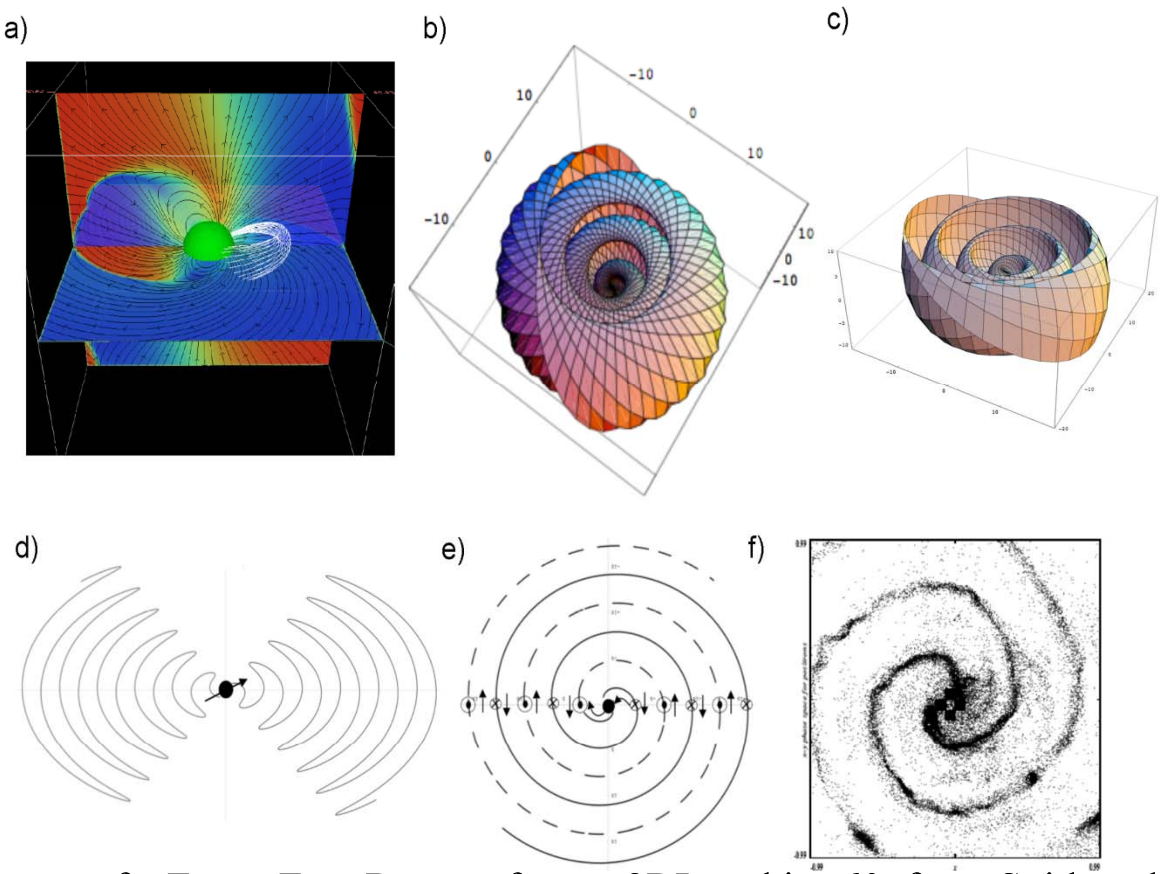

a) Magnetic Geometry of a Force-Free Rotator for r < 2RL and i = 60, from Spitkovsky (2006). The rapid transition to inclined split monopole field geometry for r > RL is apparent. b) Geometry of the current sheet from the split monopole model for i = 60, r > RL. For clarity, only one of the two spirally wound current sheets is shown. As i=90, the sheets almost completely enclose the star; for r>RL, the spirals are tightly wrapped and the current sheet surfaces closely approximate nested spheres. c) One sheet for i=30, shown for clarity. d) Meridional cross section of the current sheet for i = 60. e) Equatorial cross section snapshot of the current sheet, showing the two arm spiral form. The arrows show the local directions of the magnetic field; the dots and crosses show the direction of the current flow.

Collision of laser collisionless plasma jets

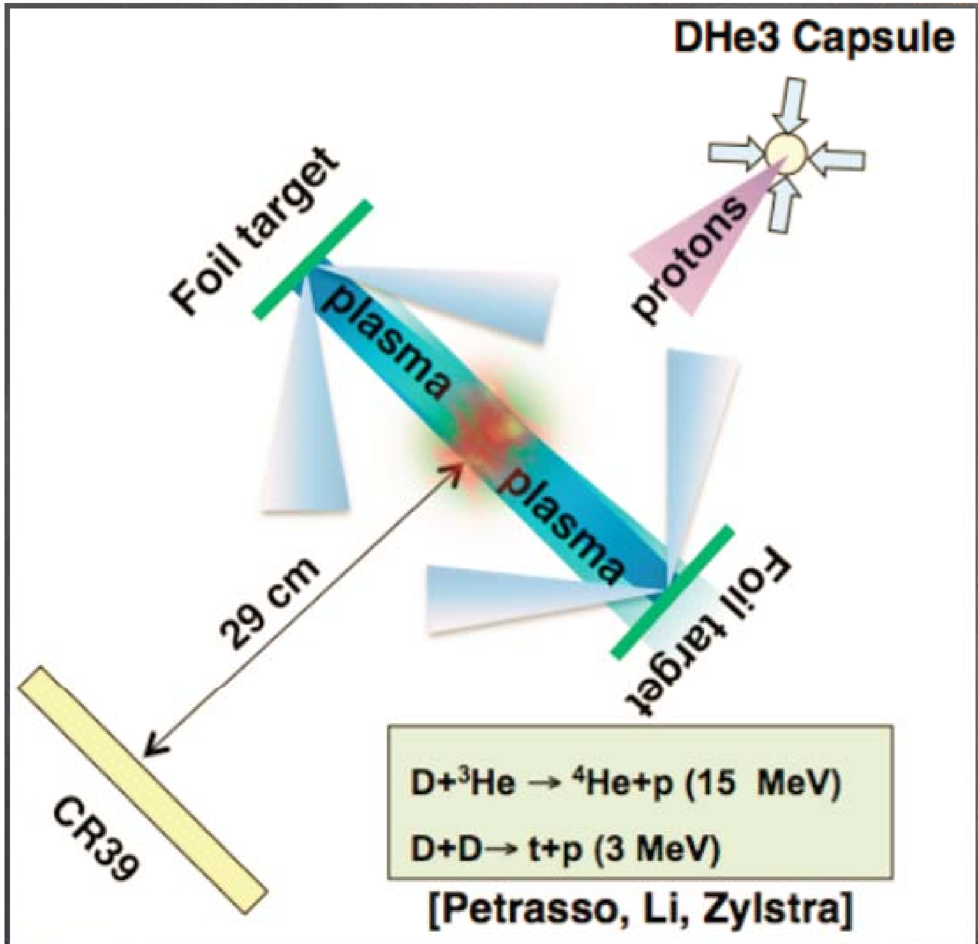

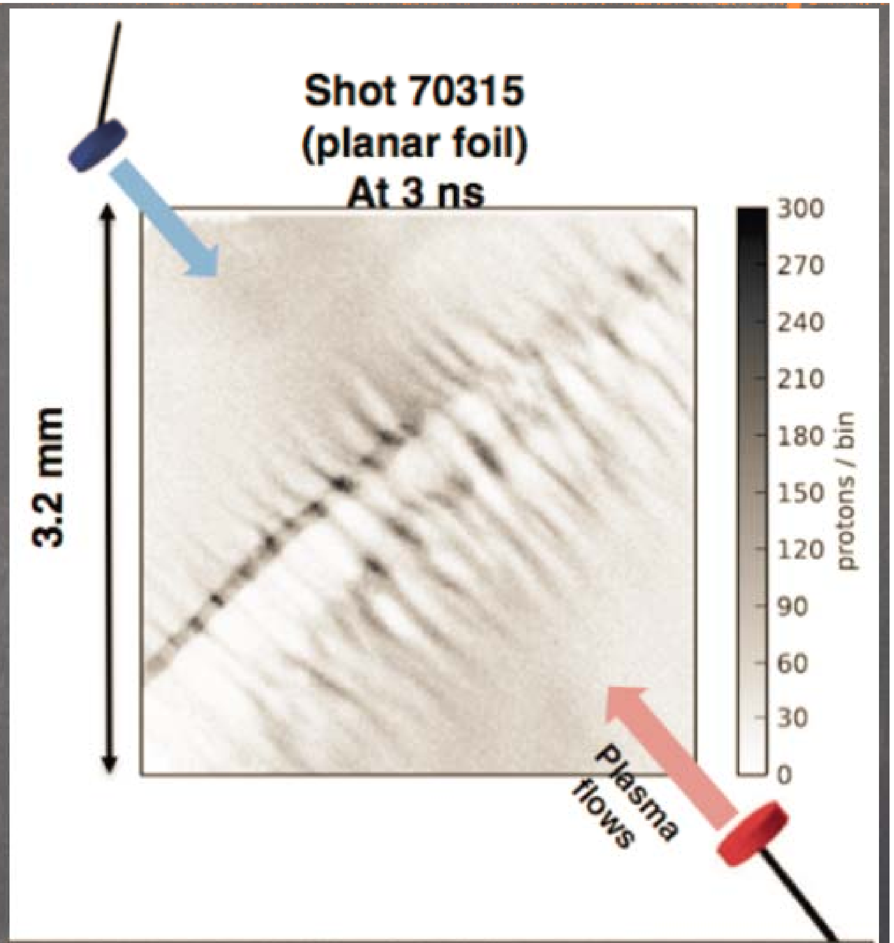

- First clearly seen filamentation from DHe3 capsule implosion protons. Later confirmed that same filamentation is seen with EP protons on Omega

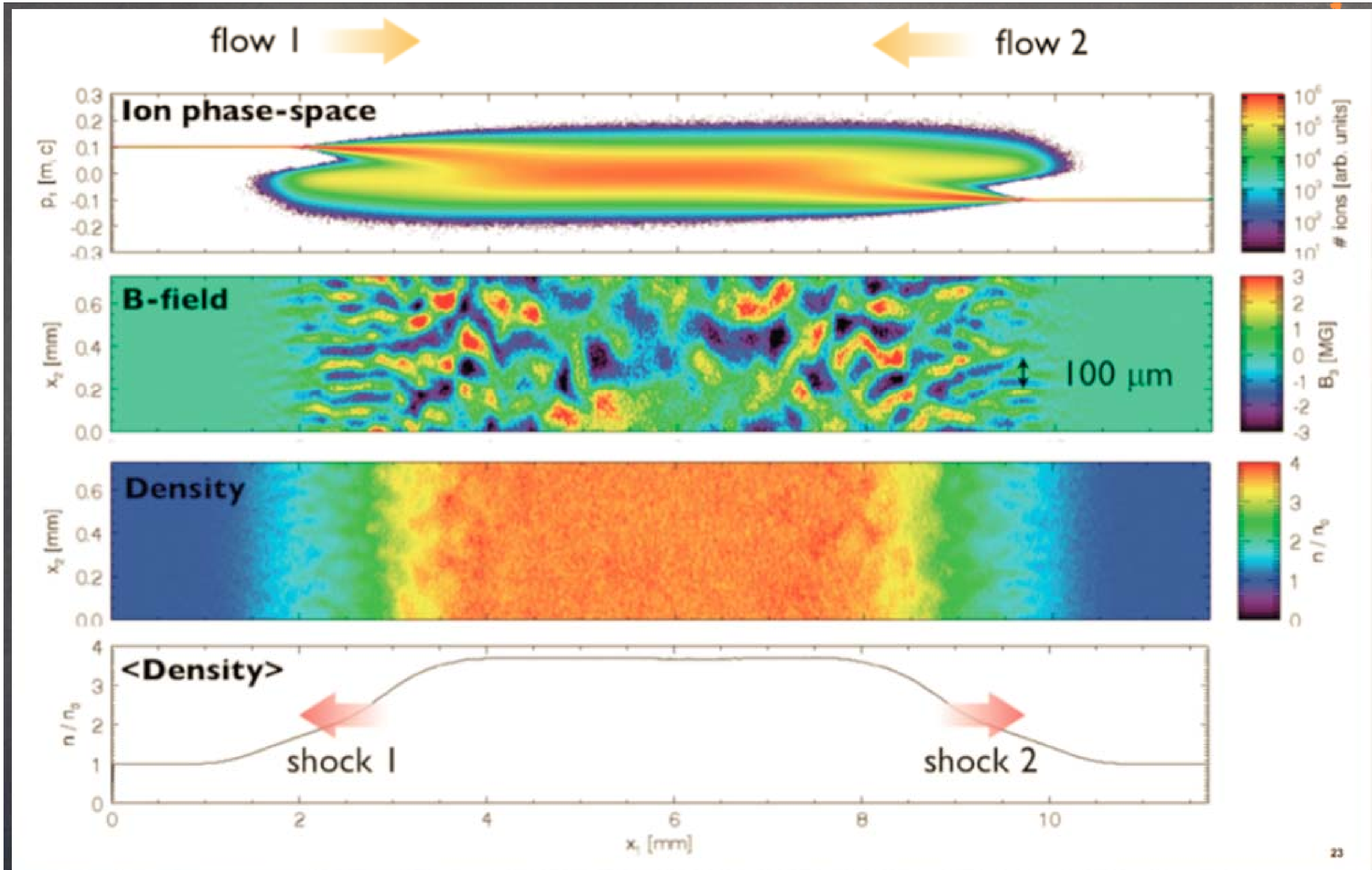

PIC simulation with OSIRIS code (Fiuza)

Higher density allows to have > 300 ion skin depths between targets.

Numerical simulations of magnetic structure formation

Particle-in-cell experiments in 2D and 3D

- A. Pukhov, Rep. Prog. Phys. 2003, **66**, 47.
- L. Silva *et al*, ApJ 2003, **596**, L121.
- F. Califano, D.D. Sarto, F. Pegoraro, PRL **96**, 105008 (2006).
- K.-I. Nishikawa, C.B. Hededal *et al*., ApJ **642**, n. 2, 1267 (2006).
- T.N. Kato, Phys. Plasmas **12**, 080705 (2005).
- A. Spitkovsky, ApJ **673**, 1, L39 (2008); U. Keshet *et al*., ApJ **693**, L127 (2009); A. Spitkovsky, L. Sironi, ApJ 698.2 (2009).
- Haugbolle, ApJ Lett. **739**, L42 (2011)
- H.-S. Park, D.D. Ryutov, J.S. Ross, High Energy Density Physics **8**, 38 (2012); **9**, 192 (2013).

Alfven current and filament self-limitation

$$I_A = \frac{mc^3}{e}\frac{v}{c}\gamma$$

$$\frac{r}{r_H} = \frac{2I}{I_A}$$

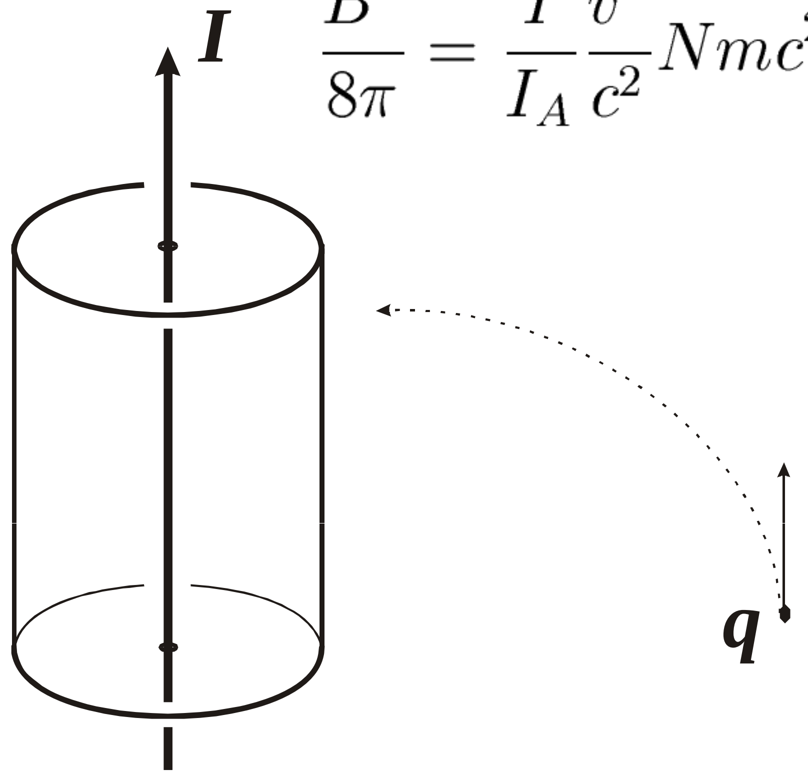

$$\frac{B^2}{8\pi} = \frac{I}{I_A}\frac{v^2}{c^2}Nmc^2\gamma$$

$$I \sim I_A \cdot \frac{D}{r_{H\min}}$$

$$\frac{B^2}{8\pi} < Nmc^2\gamma$$

Weibel instability

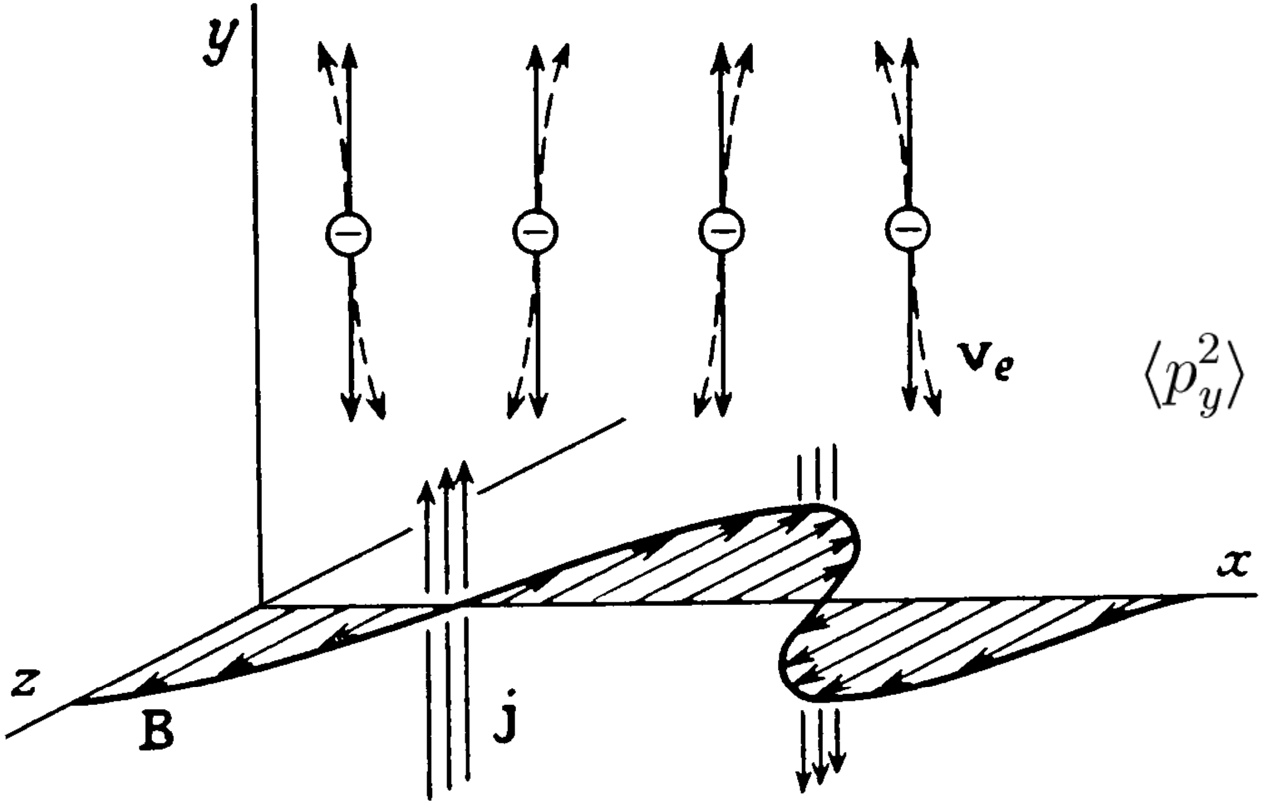

$$\langle p_y^2 \rangle > \langle p_x^2 \rangle$$

Highly anisotropic velocity distributions are unstable

$$\max(\mathrm{Im}\,\omega) \sim \omega_p/\sqrt{\gamma}$$

Dispersion relation

$$1 - \frac{c^2k^2}{\omega^2} + \sum_\alpha \frac{4\pi e_\alpha^2}{m_\alpha \omega^2} \int \left[\frac{p_y k_x}{\gamma_a m_\alpha} \frac{\partial f_{0\alpha}}{\partial p_x} + \right.$$

$$\left. + \left(\omega - \frac{\mathbf{kp}}{\gamma_a m_\alpha} \right) \frac{\partial f_{0\alpha}}{\partial p_y} \right] \frac{p_y}{(\omega - \mathbf{kp}/\gamma_a m_\alpha)} \frac{d^3\mathbf{p}}{\gamma_a} = 0$$

Typical growth rate graph

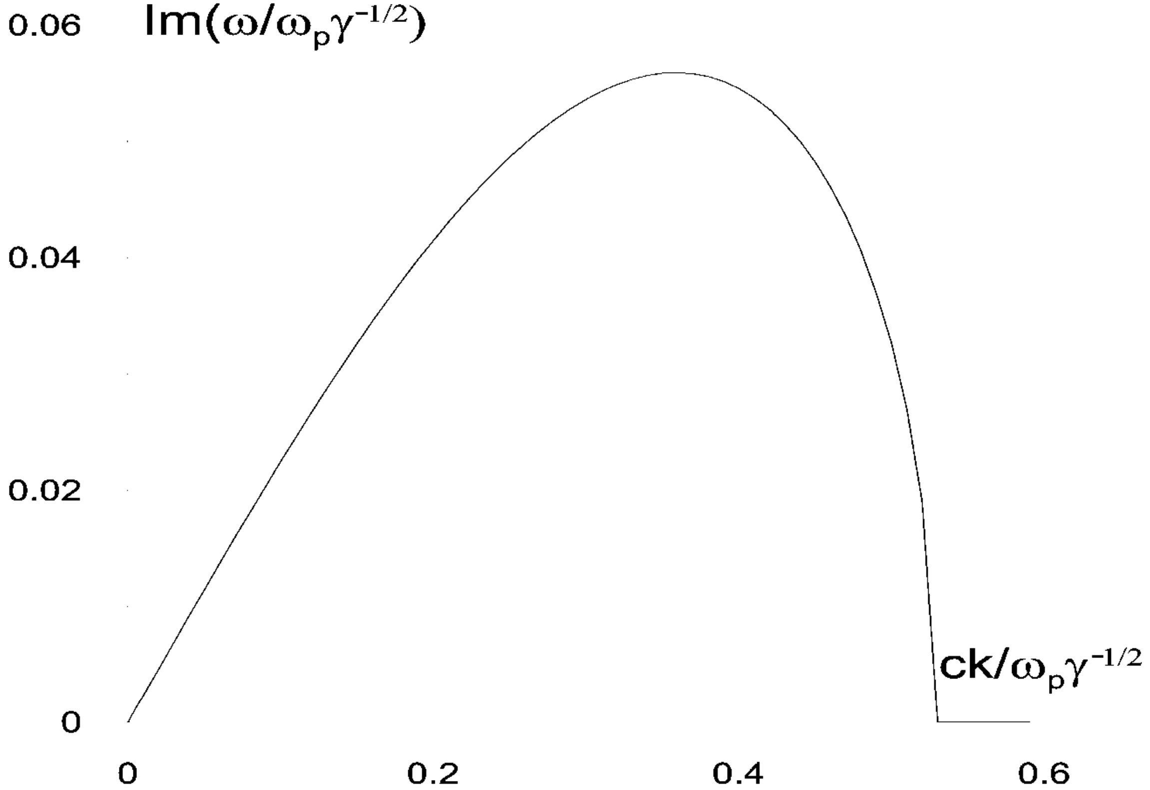

- The instability is aperiodic, $\mathrm{Re}\,\omega = 0$
- Clearly defined spatial scale, $c\sqrt{\gamma}/\omega_p << l_{free\ path}$

Instability condition

$$\omega = 0,\ k \neq 0 \Rightarrow$$

$$\sum_\alpha \frac{e_\alpha^2}{m_\alpha} \int \left[1 + \frac{p_y^2 k^2}{(\mathbf{kp})^2} \right] \frac{f_{0\alpha}}{\gamma_a} d^3\mathbf{p} < 0$$

$$\langle p_y^2 \rangle > \langle p_x^2 \rangle$$

Nonlinear evolution

- Quasineutrality
- Magnetic energy can approach equipartition
- Current filaments merge due to Ampère force
- Spatial scale increases
- Slow magnetic field decay
- Metastable configurations

Equal treatment of relativistic and non-relativistic plasma

$$\langle B^2/8\pi\rangle \lesssim \langle(\gamma-1)Nmc^2\rangle$$

The Harris current sheet solution

$$f_{e,i} = \frac{N(x,z)}{(2\pi m_{e,i} T_{e,i})^{3/2}} \exp\left(\frac{-p_x^2 - (p_y - m_{e,i} V_{e,i})^2 - p_z^2}{2 m_{e,i} T_{e,i}} \right)$$

$$\mathbf{B} = \nabla \times \mathbf{A}$$

$$V_e, V_i = \mathrm{const}$$

$$V_e/T_e = V_i/T_i$$

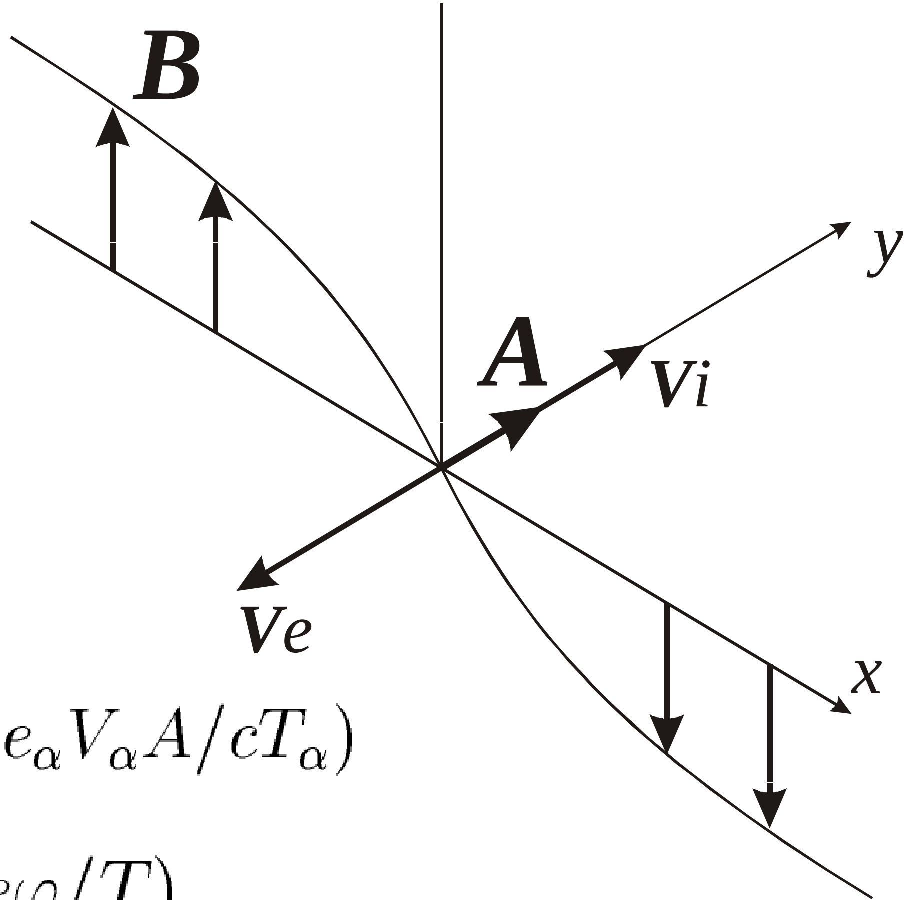

$$\Delta A = -\frac{4\pi}{c} \sum_\alpha e_\alpha N_{0\alpha} V_\alpha \exp\left(e_\alpha V_\alpha A / c T_\alpha \right)$$

$$\Delta \varphi = 4\pi \rho, \qquad \rho \sim \exp(-e\varphi/T)$$

Balance of forces: $e_\alpha E_\alpha = T_\alpha \nabla N_\alpha$

Generalizations of Harris' solution,
mainly based on modified Maxwellian distributions

- Harris, 1962
- Fadeev et al., 1965
- Hoh, 1966
- Alpers, 1969
- Kan, 1973
- Channell, 1976
- Attico and Pegoraro, 1999
- Manakova et al., 2000
- Brittnacher and Whipple, 2002
- Schindler and Birn, 2002
- Mottez, 2003
- Yoon and Lui, 2005
- Zelenyi et al., 2006
- Suzuki and Shigeyama, 2008
- Janaki, Dasgupta and Yoon, 2012, 2014

and also on kappa distributions

$$f^{\kappa}(\vec{v}) = \frac{n}{2\pi(\kappa v_{\kappa}^{2})^{3/2}} \frac{\Gamma(\kappa+1)}{\Gamma\left(\kappa-\frac{1}{2}\right)\Gamma\left(\frac{3}{2}\right)} \left(1+\frac{v^2}{\kappa v_{\kappa}^{2}}\right)^{-(\kappa+1)}$$

- Fu, Hau, 2005
- Yoon, Lui, 2006
- Vasko, 2013

Basic nonlinear equations describing stationary self-consistent current configurations in collisionless multicomponent plasma

$$\mathbf{p}\frac{\partial f_\alpha}{\partial \mathbf{r}} + \frac{e_\alpha}{c}[\mathbf{p} \times [\nabla \times \mathbf{A}]]\frac{\partial f_\alpha}{\partial \mathbf{p}} = 0$$

$$[\nabla \times [\nabla \times \mathbf{A}]] = \frac{4\pi}{c}\sum_\alpha e_\alpha \int f_\alpha \frac{\mathbf{p}}{m_\alpha \gamma_a} d^3\mathbf{p}$$

V.Ju. Martyanov, Vl.V. Kocharovsky, V.V. Kocharovsky, JETP **107**, 1049 (2008);
Radiophys. Quant. Electr. **52**, n. 2 (2009);
Astronomy Lett. **36**, 396 (2010);
Phys. Rev. Lett. **104**, 215002 (2010);
Physics of Plasmas **22**, 083303 (2015).

Integrals of particle motion

$$\mathcal{E} = c\sqrt{m^2c^2 + p^2}$$

$$P_y = p_y + \frac{e}{c}A_y$$

$$p_z$$

$$f = f(\mathcal{E}, P_y, p_z)$$

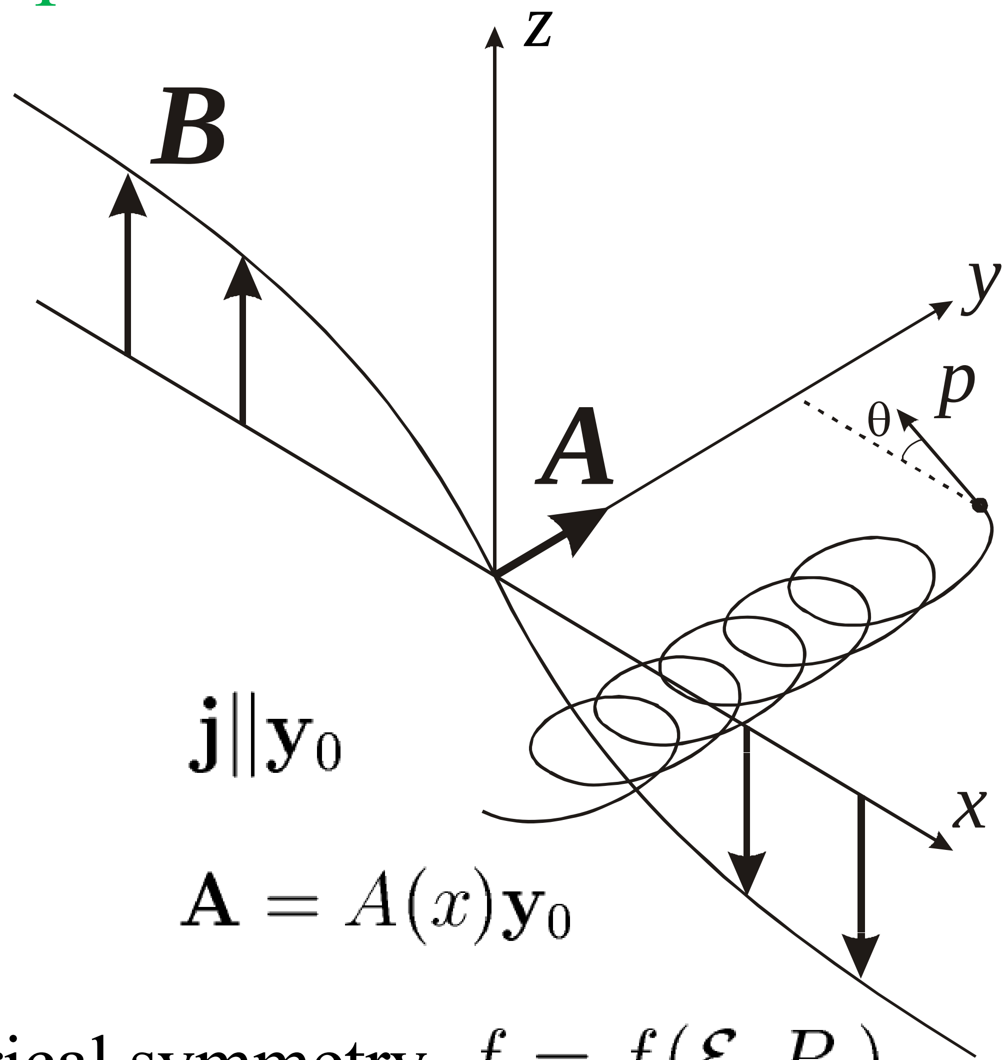

Special case of PDF: cylindrical symmetry, $f = f(\mathcal{E}, P_y)$

1D charged current structures with sheared magnetic field

$$\frac{d^2\varphi}{dx^2} = -4\pi \sum_\alpha e_\alpha \iiint f_\alpha \left(\gamma_\alpha m_\alpha c^2 + e_\alpha \varphi,\ p_y + \frac{e_\alpha A_y}{c},\ p_z + \frac{e_\alpha A_z}{c}\right) d^3\mathbf{p}$$

$$\frac{d^2 A_{y,z}}{dx^2} = -\frac{4\pi}{c} \sum_\alpha \iiint \frac{e_\alpha p_{y,z}}{m_\alpha \gamma_\alpha} f_\alpha \left(\gamma_\alpha m_\alpha c^2 + e_\alpha \varphi,\ p_y + \frac{e_\alpha A_y}{c},\ p_z + \frac{e_\alpha A_z}{c}\right) d^3\mathbf{p}$$

$$\frac{d^2 A_{y,z}}{dx^2} = -\frac{4\pi}{c} \frac{dP_{xx}}{dA_{y,z}}$$

$$\frac{d^2\varphi}{dx^2} = 4\pi \frac{dP_{xx}}{d\varphi}$$

component of the pressure tensor

$$P_{xx} = \sum_\alpha N_\alpha \iiint f_\alpha p_x v_x d^3\mathbf{p}$$

Charge

- Morozov, Soloviev, 1961
- Yoon, Lui, 2004, 2006
- Cremaschini et al, 2010, 2012
- Tautz, Lerche, 2011

Shear

- Channell, 1976
- Mahajan, 2000
- Neukirch, 2009
- Ghosh, Janaki, Dasgupta, 2014

1D current sheets with sheared magnetic field

$$\varphi \equiv 0 \qquad \frac{B_y^2 + B_z^2}{8\pi} + P_{xx} = \text{const}$$

$$f_\alpha = f_\alpha^{(y)}\left(\gamma_\alpha m_\alpha c^2,\ p_y + \frac{e_\alpha A_y}{c}\right) + f_\alpha^{(z)}\left(\gamma_\alpha m_\alpha c^2,\ p_z + \frac{e_\alpha A_z}{c}\right)$$

$$U^{(y,z)}(A_{y,z}) = 4\pi P_{xx}^{(y,z)} + \text{const}$$

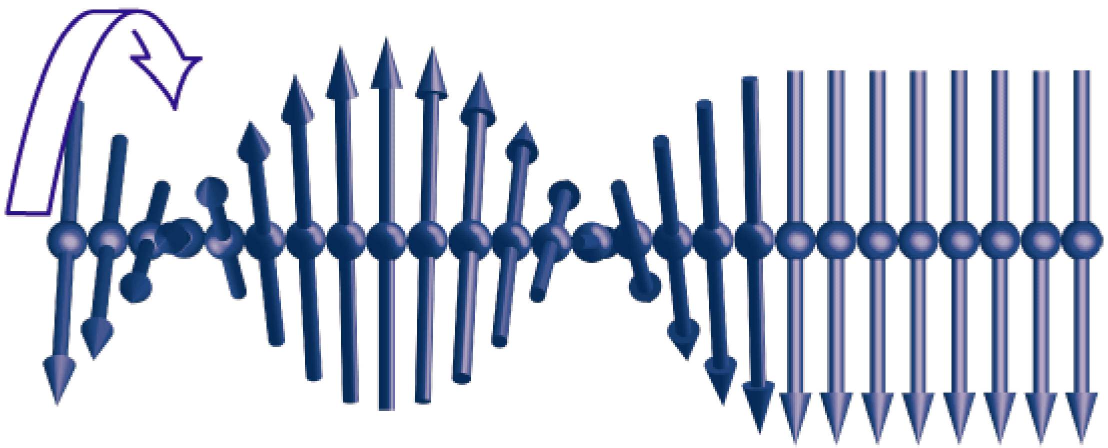

1D superposition of two current sheets with orthogonal currents and cylindrically symmetrical particle distributions $f^{(x)}$, $f^{(y)}$

Grad-Shafranov equation and PDF decomposition 1

$$f_\alpha\left(P_y, \mathcal{E}\right) = \sum_j f_{\alpha j}(\mathcal{E}) \left(\frac{P_y}{m_\alpha c}\right)^j$$

$$\frac{\partial^2 A}{\partial x^2} + \frac{\partial^2 A}{\partial z^2} = -\frac{\partial U}{\partial A}$$

$$U = -8\pi^2 m_\alpha^2 c^3 \sum_{j=0}^{\infty} \int f_{\alpha j}(\mathcal{E}) Q_j \left(\frac{e_\alpha A}{m_\alpha c^2}, \frac{p}{m_\alpha c}\right) \frac{p}{\gamma} dp$$

$$Q_j(A,p) = \frac{(A+p)^{j+2}\left[p(j+2) - A\right] + (A-p)^{j+2}\left[p(j+2) + A\right]}{(j+1)(j+2)(j+3)}$$

Grad-Shafranov equation and PDF decomposition 2

$$f_\alpha(\mathcal{E}, P_y) = \exp\left(\zeta_\alpha \frac{P_y}{m_\alpha c}\right) \sum_{i=0}^{d} f_{\alpha i}(\mathcal{E}) \left(\frac{P_y}{m_\alpha c}\right)^i$$

$$\frac{\partial^2 A}{\partial x^2} + \frac{\partial^2 A}{\partial z^2} = -\frac{dU}{dA}$$

$$U = \sum_\alpha \exp\left(\frac{\zeta_\alpha e_\alpha A}{m_\alpha c^2}\right) \sum_{j=0}^{d} A^j \left\{\sum_{i=j}^{d} \int f_{\alpha i}(\mathcal{E}) \left[Y_{\alpha ij}(p) - Y_{\alpha ij}(-p)\right] dp\right\}$$

$$Y_{\alpha ij}(p) = \exp\left(\frac{\zeta_\alpha p}{m_\alpha c}\right) \frac{4\pi^2 e_\alpha^j p \left(-\zeta_\alpha\right)^{j-i-3} i!}{\gamma_\alpha m_\alpha^{j-2} c^{2j-3} j!(i-j)!} \cdot$$

$$\cdot \left(\exp(q)\Gamma(i-j+1, q) \left[(i-j+2)(i-j+1) - q^2\right] + q^{i-j+2} + (i-j+2)q^{i-j+1}\right)$$

$q = -\zeta_\alpha p / m_\alpha c$ $\quad$ $\exp(q)\Gamma(i-j+1, q)$ — polynomial of order $i-j$

Harmonic solution of nonlinear problem (d=2)

$$\Delta_\perp A + k^2 A = 0$$

$$k^2 = \frac{32\pi^2}{3} \int f_2(\mathcal{E}) \frac{e^2 p^4}{m^3 c^4 \gamma} dp$$

$$A = A_{\max} \cos(kx)$$

$$\frac{\langle W_B \rangle}{\langle W_e \rangle} = \frac{1}{3} \frac{\int f_2(\mathcal{E})(v^2/c^2)\gamma p^2 dp}{\int f_2(\mathcal{E})\gamma p^2 dp + \frac{2}{3}\int f_2(\mathcal{E}) p^2 c^2 \gamma p^2 \; dp / e^2 A_{\max}^2}$$

$$\frac{\langle W_B \rangle}{\langle W_e \rangle} = \frac{1}{3} \cdot \frac{1}{1 + \frac{2}{3}\frac{p^2 c^2}{e^2 A_{\max}^2}} \cdot \frac{v^2}{c^2} < \frac{1}{3}$$

$$f(\mathcal{E}, P_y) \propto \exp(-\mathcal{E}/kT) P_y^2 \qquad A = A_{\max} \sin kx$$

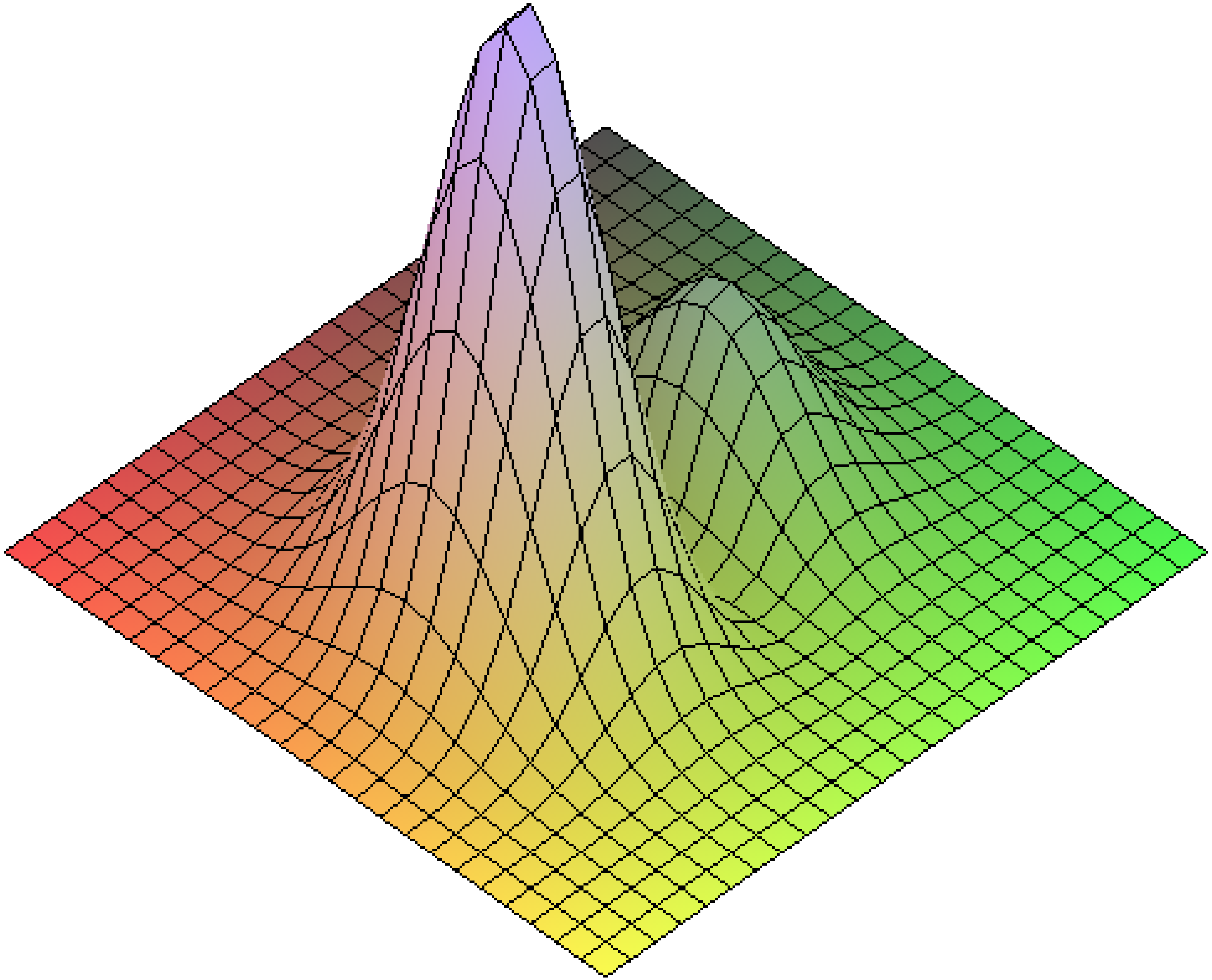

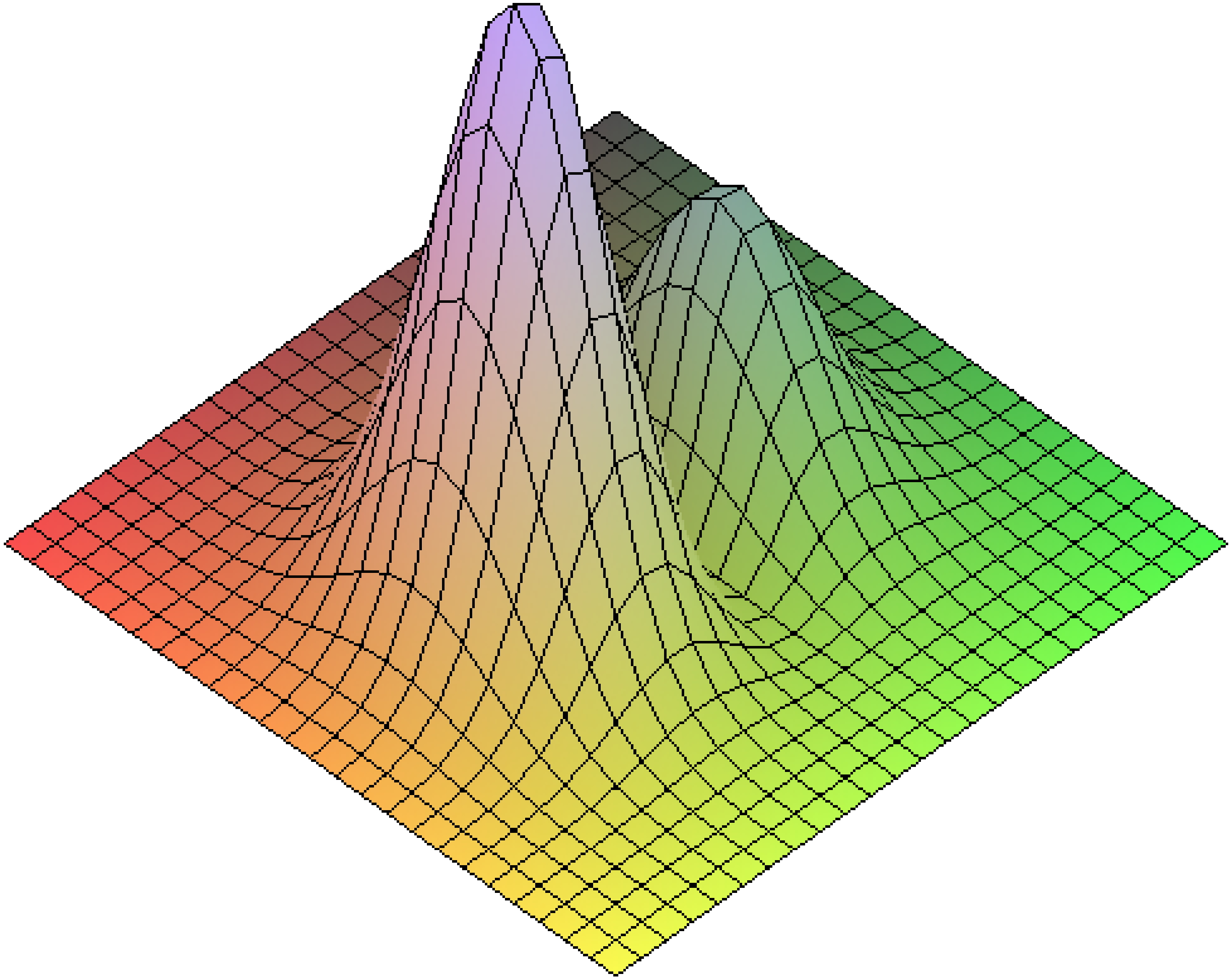

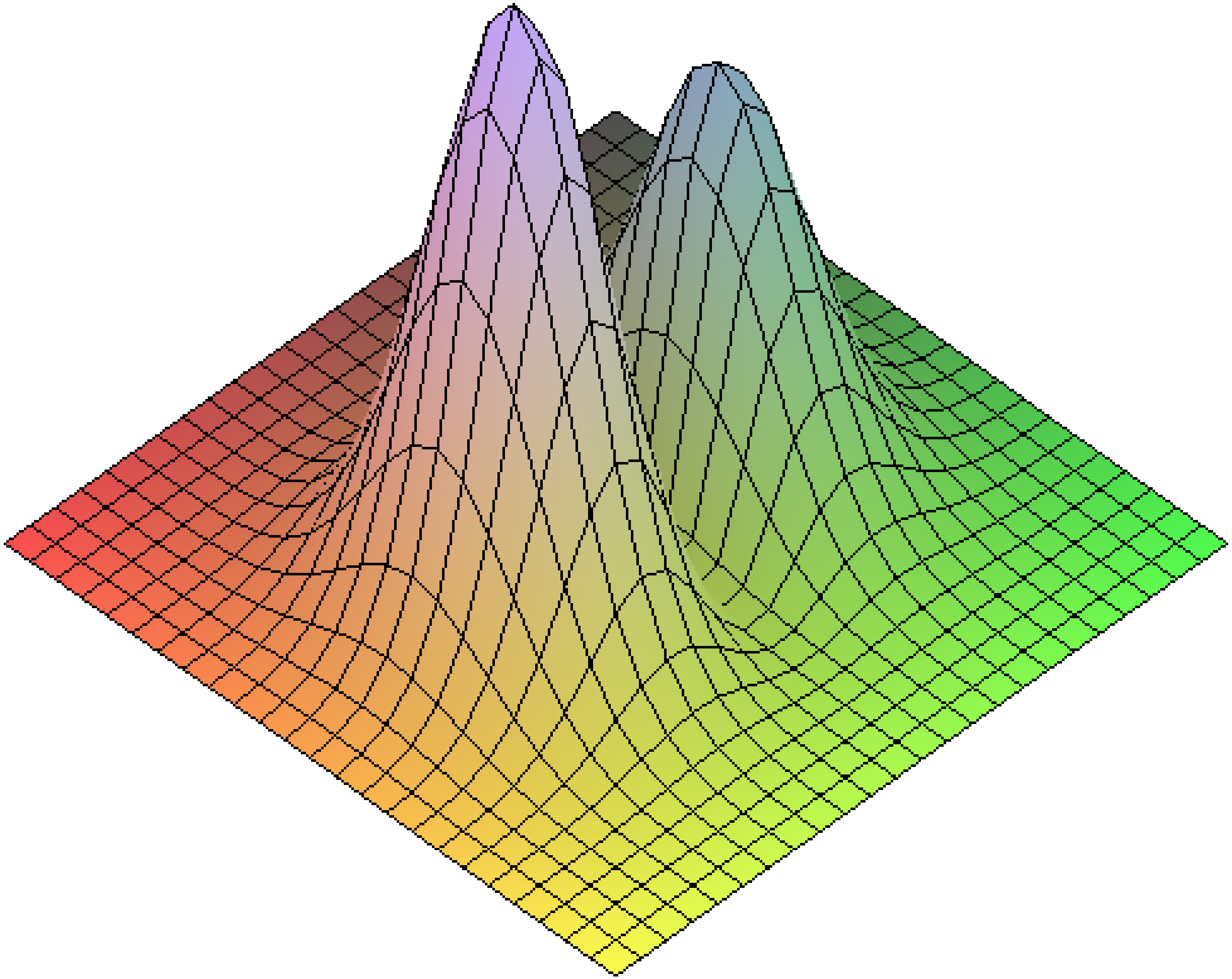

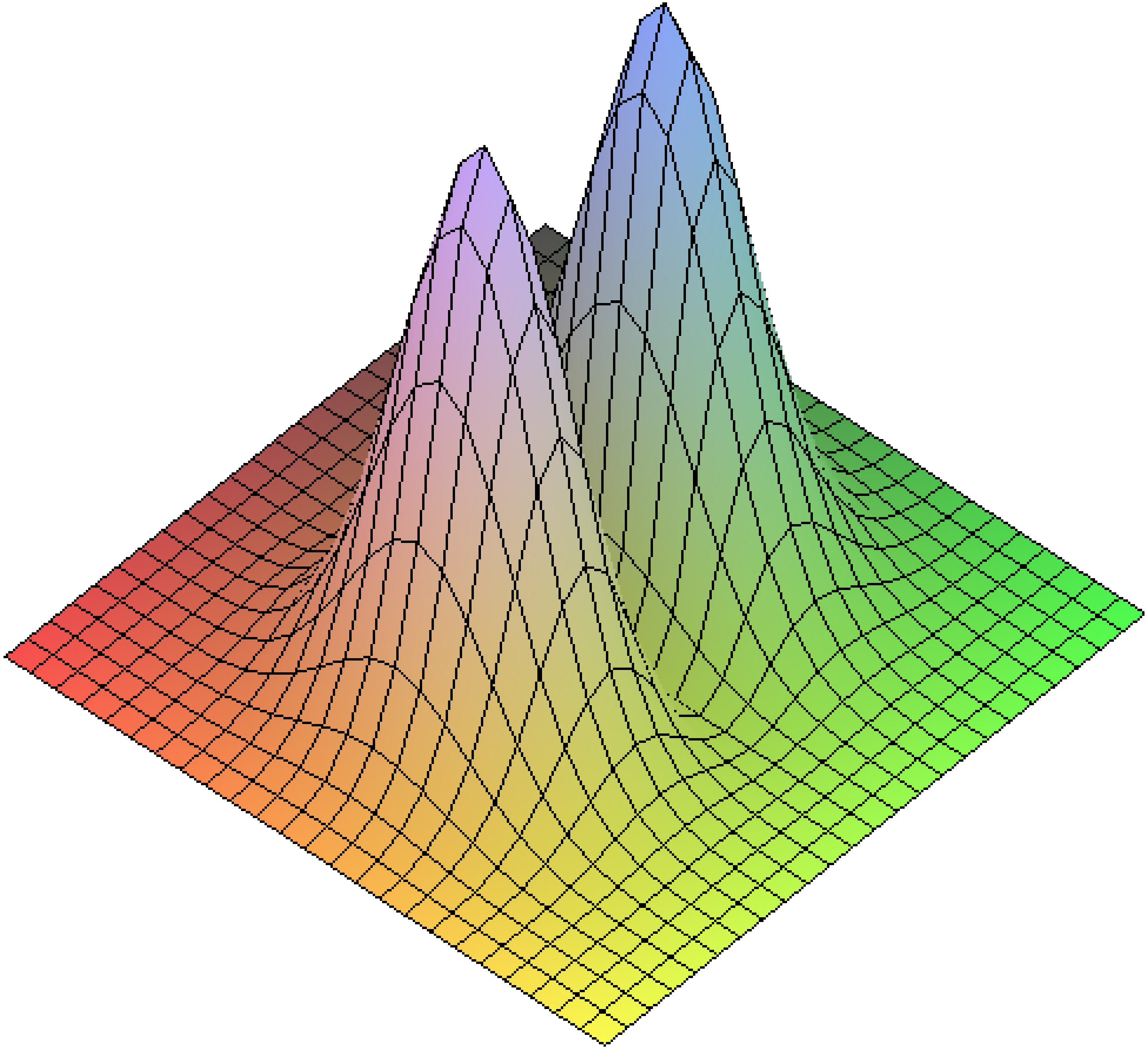

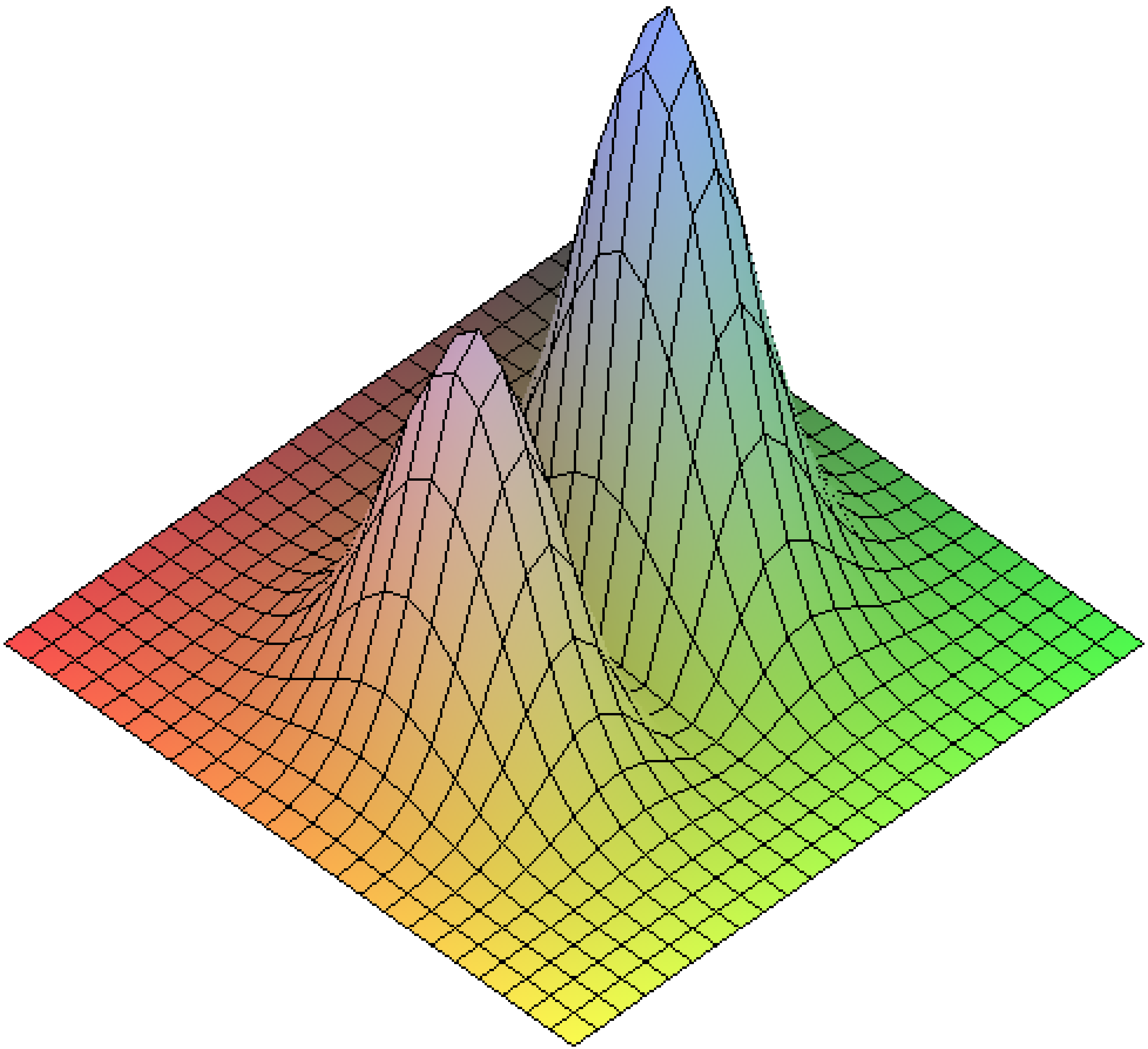

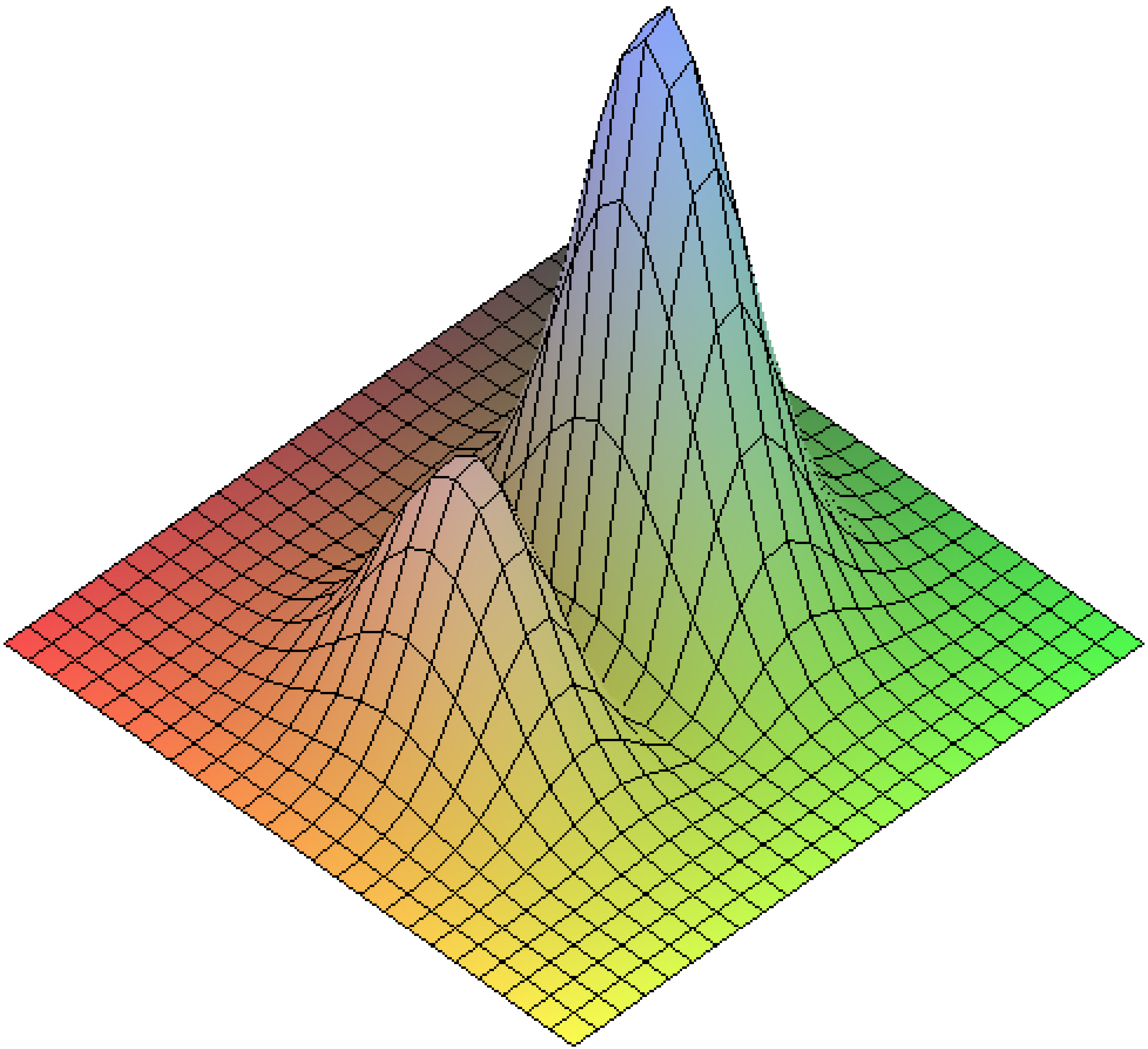

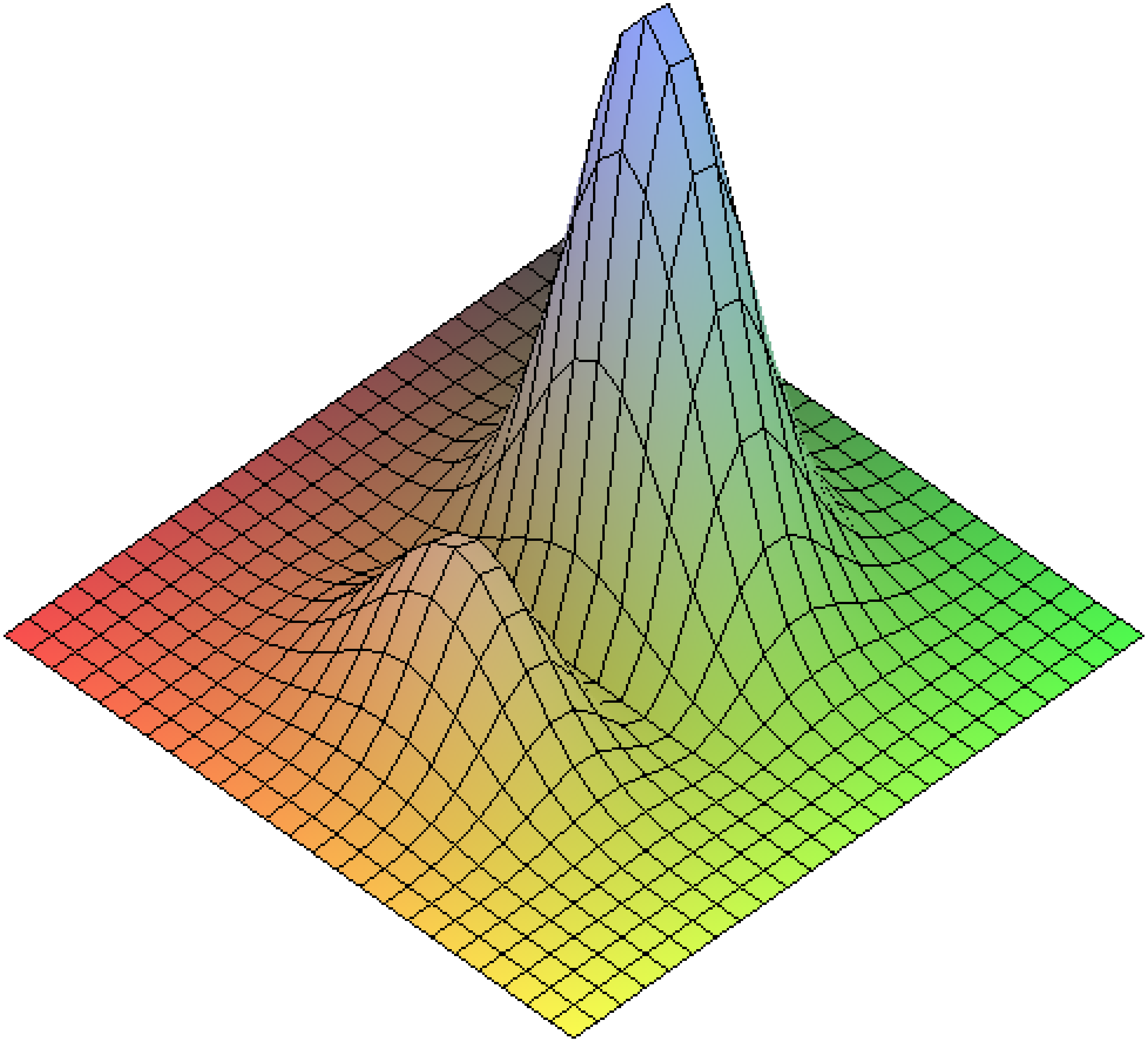

Grad-Shafranov potential and variety of solutions

$$A = A\ (x)$$

$$\frac{\partial^2 A}{\partial x^2} = -\frac{dU}{dA}$$

$$x\,(A\ ) = \int^{A_y} \frac{dA'}{\sqrt{2U_0 - 2U(A')}}$$

Periodic sheets

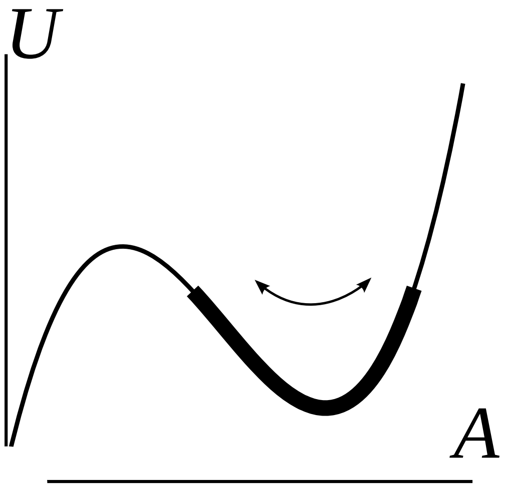

Isolated sheets (I ≠ 0)

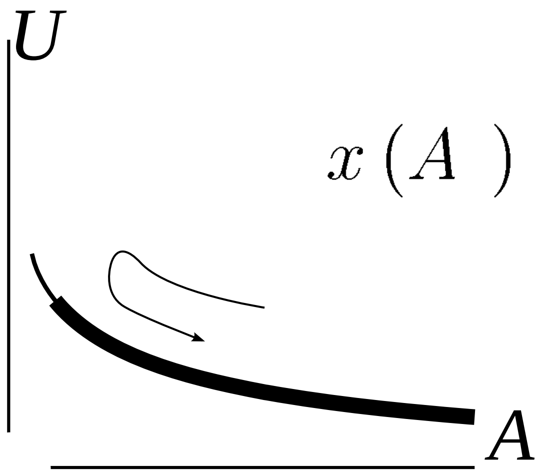

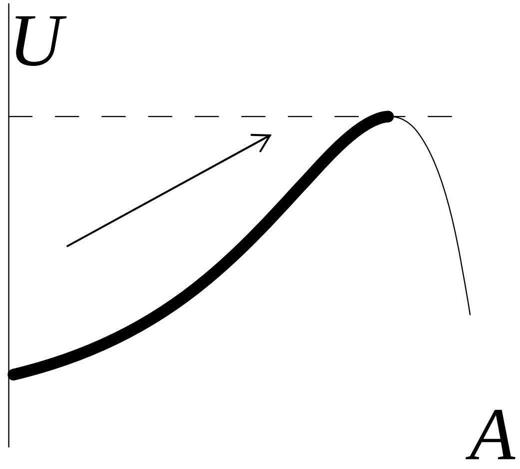

Boundary sheets

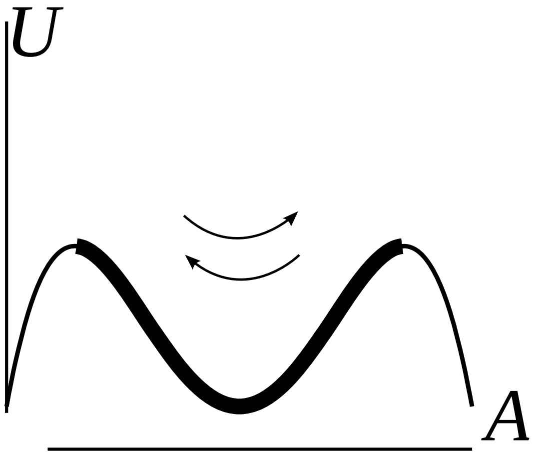

Double sheets

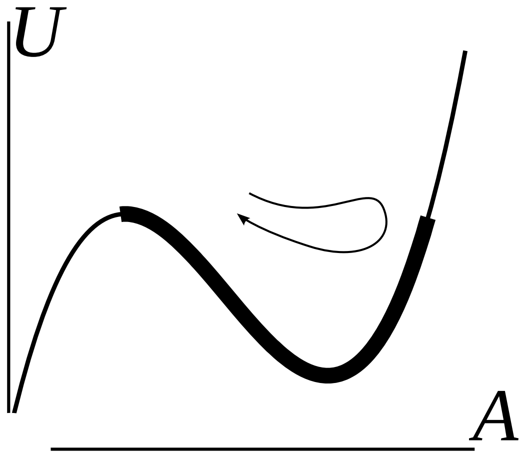

Symmetrical shielded sheets

Generalized relativistic Harris current sheet (d=0, ζ≠0)

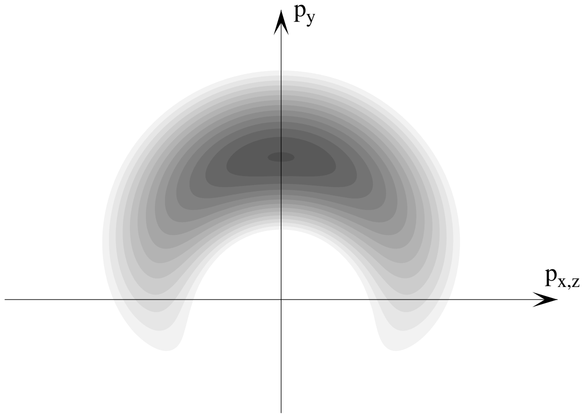

$$A = -2A_0 \ln\cosh\left(\sqrt{\alpha/2A_0}\;x\right) + \mathrm{const}$$

$$B = -A_0\sqrt{2\alpha/A_0}\tanh\left(\sqrt{\alpha/2A_0}\;x\right)$$

$$N_e - N_0 \propto \cosh^{-2}\left(\sqrt{\alpha/2A_0}x\right)$$

$$F = F_0(p)\exp\left(\frac{cp_y/e + A}{A_0}\right)$$

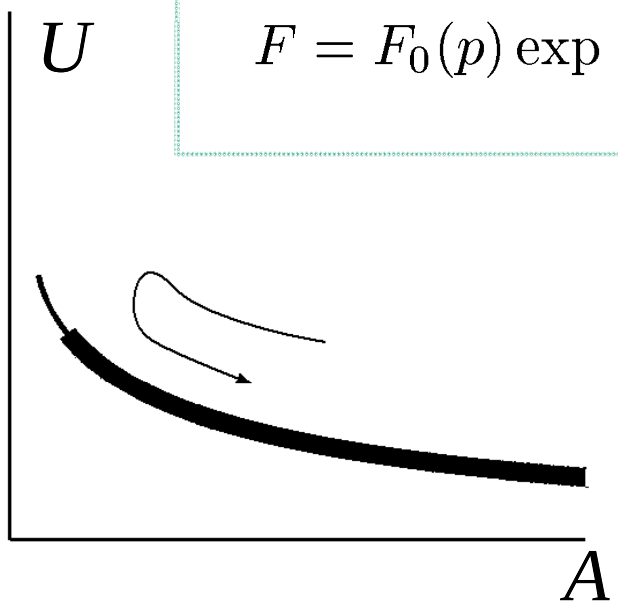

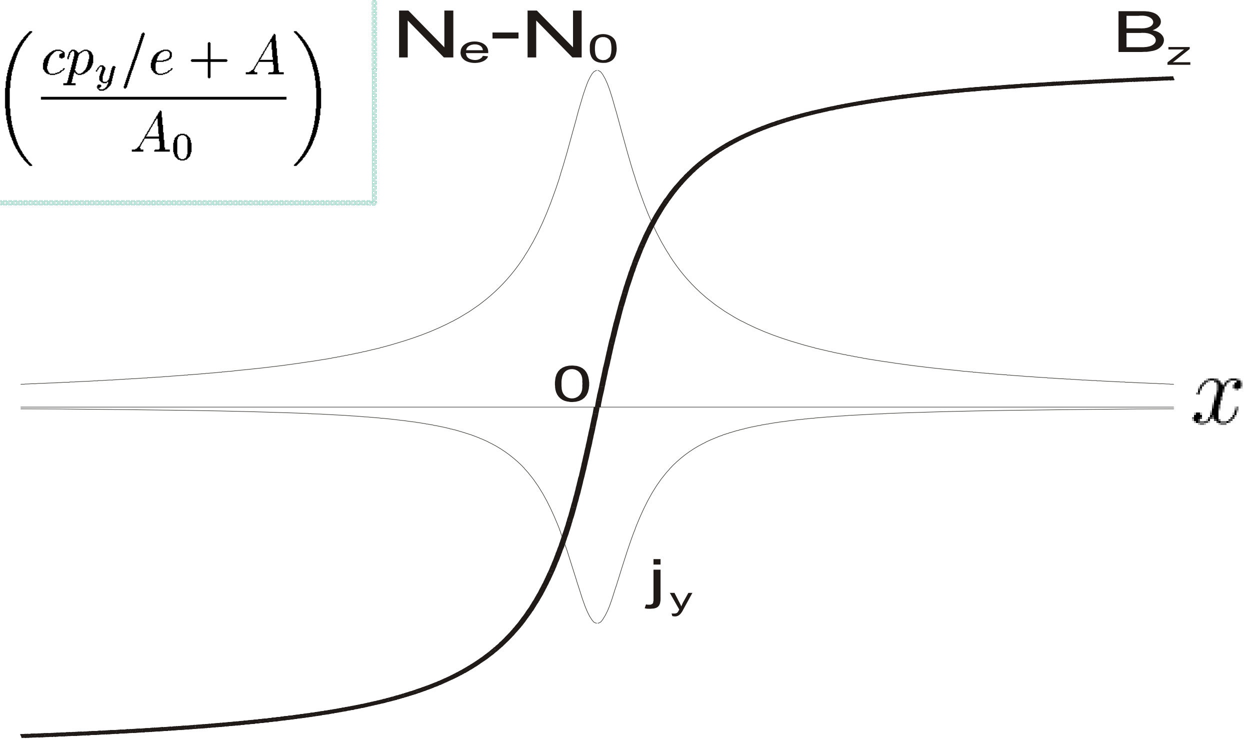

Bifurcated current sheet with two peaks

$$\frac{d^2 A_y}{dx^2} = -\frac{W_1}{A_0}\exp\left(\frac{A_y}{A_0}\right) - \frac{W_2}{wA_0}\exp\left(\frac{A_y}{wA_0}\right)$$

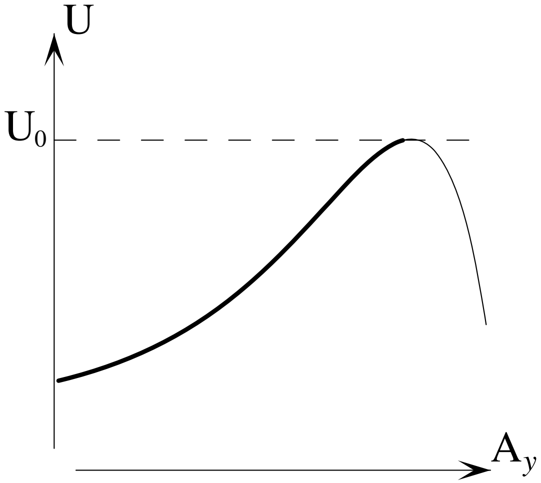

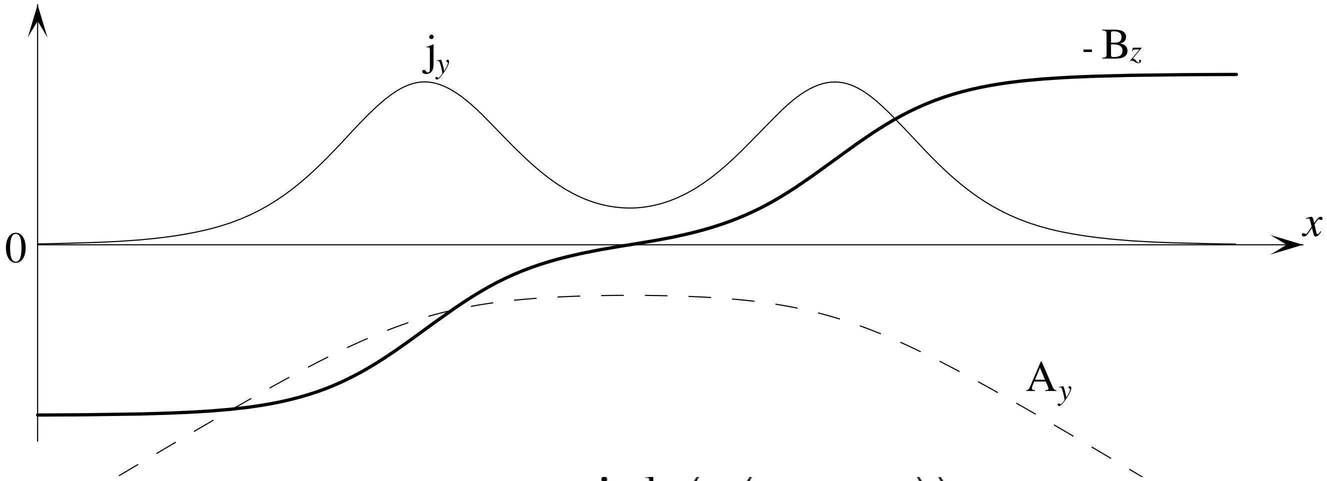

$$B_y = 2\kappa A_0 \frac{\sinh\left(\kappa(x - x_0)\right)}{\cosh\left(\kappa(x - x_0)\right) + W_2/\sqrt{W_2^2 + 2\kappa^2 A_0^2 W_0}},$$

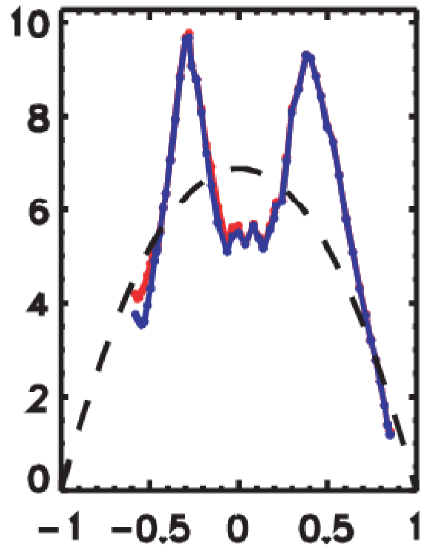

CLUSTER data

$$j_z = \frac{c\kappa^2 A_0}{2\pi} \frac{1 + \left(W_2/\sqrt{W_2^2 + 2\kappa^2 A_0^2 W_0}\right)\cosh\left(\kappa(x - x_0)\right)}{\left(\cosh\left(\kappa(x - x_0)\right) + W_2/\sqrt{W_2^2 + 2\kappa^2 A_0^2 W_0}\right)^2}$$

Shielded current sheet (two exponent PDF)

$$U = -\frac{2U_0}{\alpha}\exp\left(-\frac{A}{A_0}\right) + \frac{2U_0}{\alpha^2}\exp\left(-\frac{2A}{A_0}\right)$$

$$A = -A_0 \ln \frac{\alpha}{1 + (U_0/A_0^2)x^2}$$

Resembles Harris sheet, but with decaying magnetic field $B \sim 1/x$

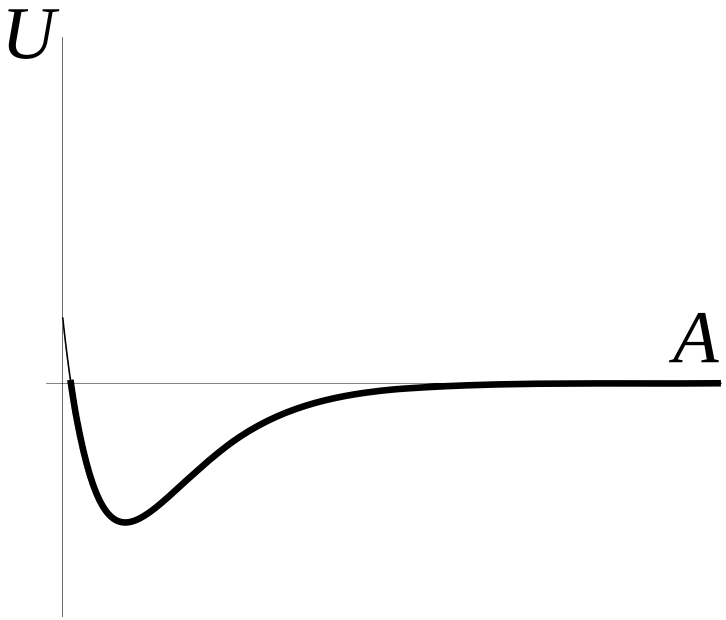

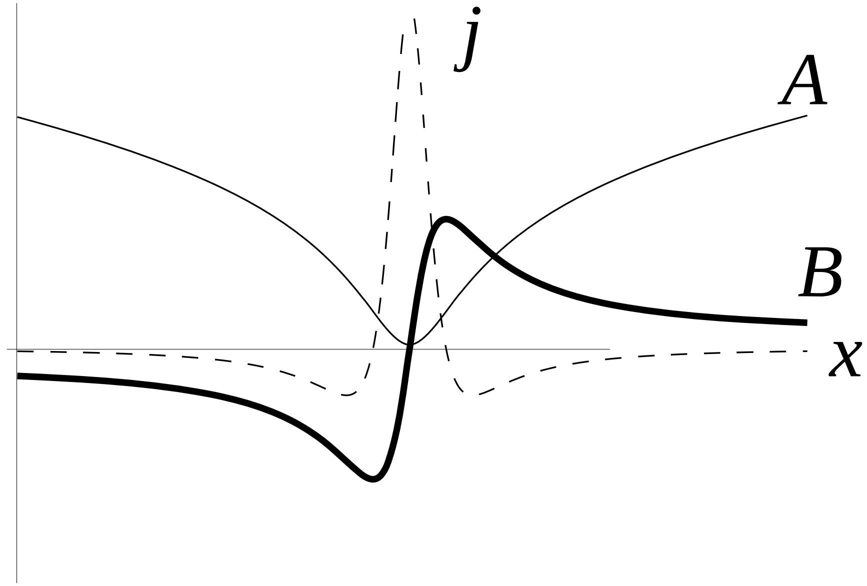

Partially or completely shielded current sheets

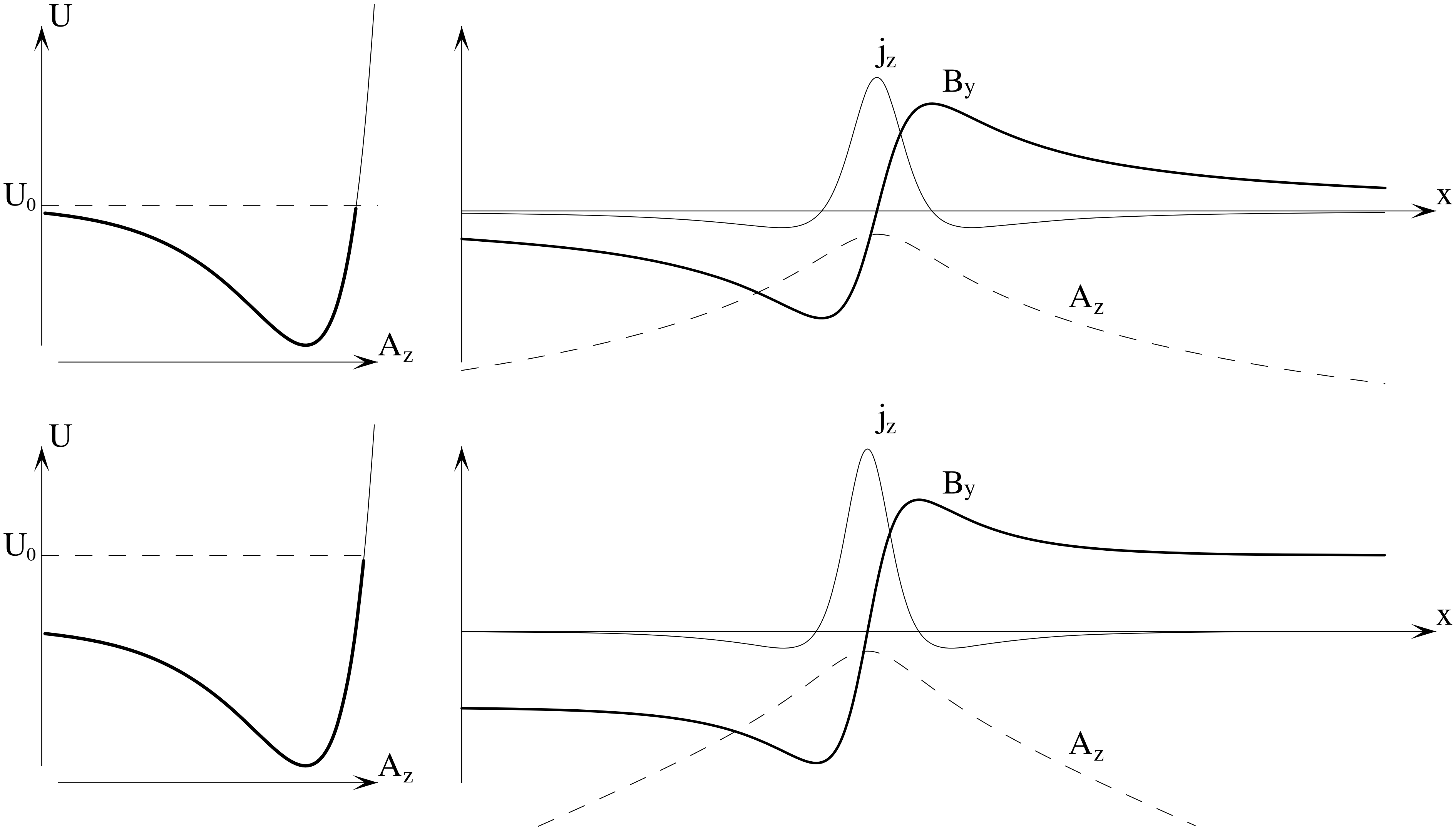

All profiles are described analytically

Shielded current sheets (Taylor order d=3)

$$A = -\frac{\sum_\alpha \int_0^\infty \hat{F}_{\alpha 2}(p)\, p^4 N_\alpha e_\alpha^2 c^2/(m_\alpha^3 \gamma_\alpha)\; dp}{\sum_\alpha \int_0^\infty \hat{F}_{\alpha 3}(p)\, p^4 N_\alpha e_\alpha^3/(m_\alpha^4 \gamma_\alpha)\; dp} \cosh^{-2}\left(\sqrt{-\sum_\alpha \int_0^\infty \frac{\hat{F}_{\alpha 2}(p)\pi^2 N_\alpha}{\gamma_\alpha}\frac{8p^4 e_\alpha^2}{3m_\alpha^3 c^4} dp\; x}\right)$$

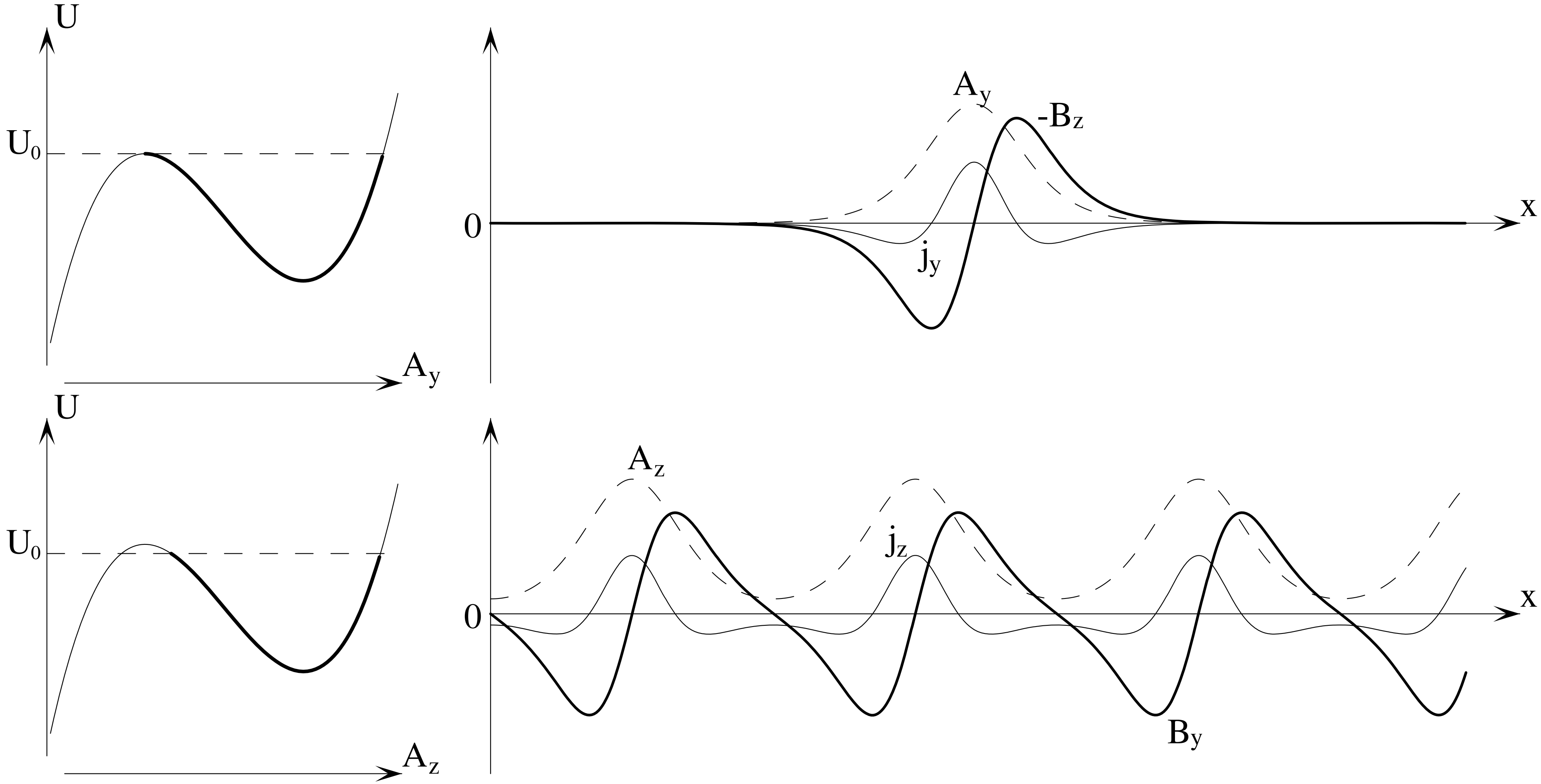

Shielded current sheet (Taylor order d=4)

$$A = (A_0/\sqrt{2})\sqrt{1 - \tanh^2\left[\left(\sqrt{-U_0}/A_0\right)x\right]}$$

$$A_0^2 = S\left(-5\sum_j \int \frac{\hat{F}_{j4}(p)}{m_j^5 c^8} e_j^4 p^4 \frac{dp}{\gamma_j}\right)^{-1}, \;\; U_0 = \frac{16\pi^2}{15c} A_0^2 S$$

$$S = \sum_j \int \frac{[5\hat{F}_{j2}(p) m_j^2 c^2 + 6\hat{F}_{j4}(p) p^2]}{m_j^5 c^5} e_j^2 p^4 \frac{dp}{\gamma_j}$$

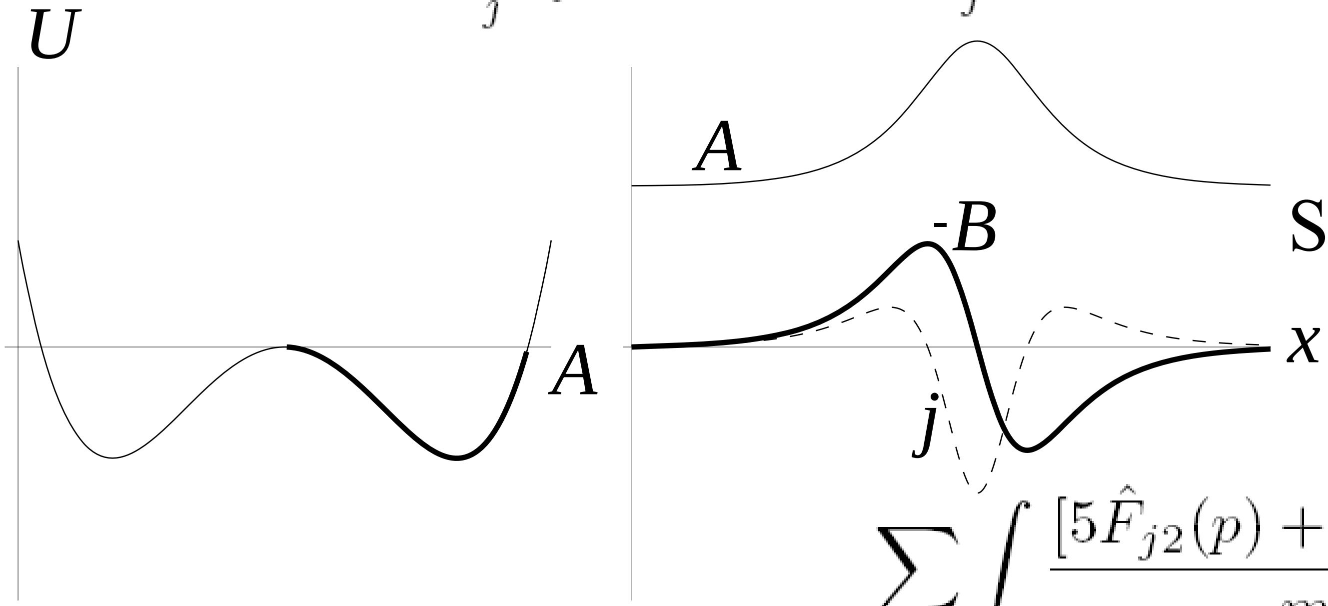

Stability conditions:

$$A_0^2 > 0$$

$$\mathbf{k} \perp \mathbf{z}, \; \mathbf{E} \| \mathbf{z}$$

$$\sum_j \int \frac{[5\hat{F}_{j2}(p) + 2\hat{F}_{j4}(p) p^2]}{m_j c} e_j^2 p^4 \frac{dp}{\gamma_j} > 0$$

$$\mathbf{k} \| \mathbf{z}, \; \mathbf{E} \perp \mathbf{z}$$

Double-scale current sheet

PDF is enriched with an exponential fraction which has a fast dependence on a vector potential A_z

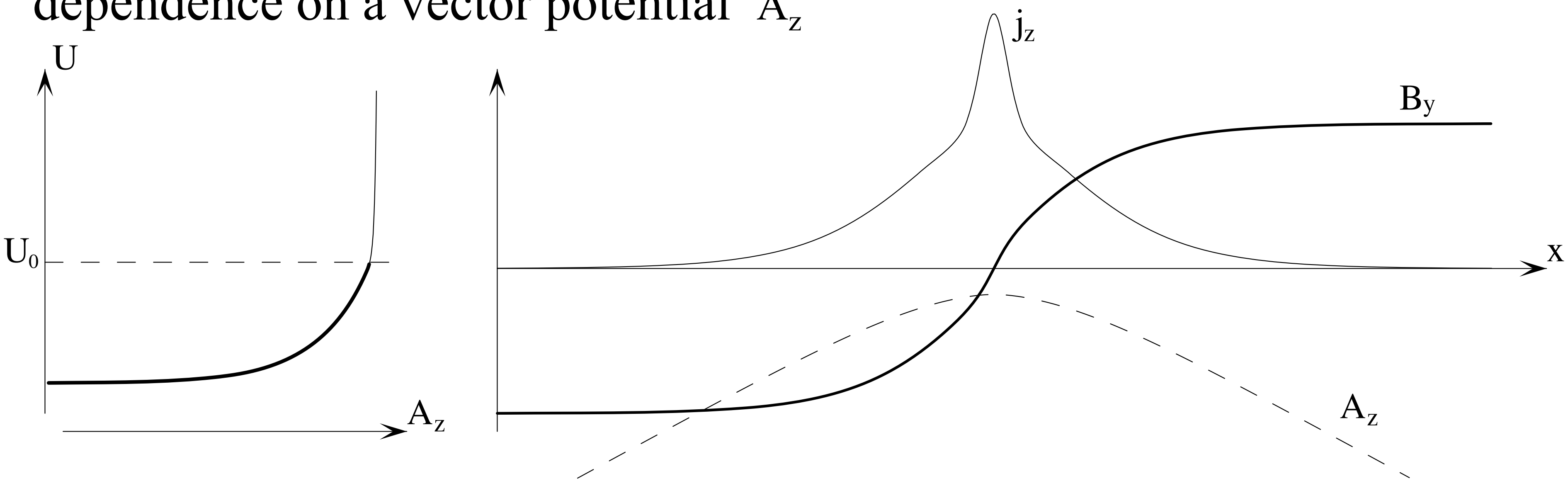

- Ratio of currents in the inner and outer layers are arbitrary.
- Particle spices in two layers may be different.
- A thin layer is similar to the Harris sheet (PDF profile is unique everywhere), a thick layer is an arbitrary symmetric one.

Pair of current sheets (d=4, ζ=0)

$$A_z = A_{\max} \tanh\left(\frac{x}{D}\right)$$

$$D = \left[\sum_\alpha \int_0^\infty \left(\hat{F}_{\alpha 2}(p)\frac{16\pi^2 N_\alpha p^4 e_\alpha^2}{3m_\alpha^3\gamma_\alpha c^4} + \hat{F}_{\alpha 4}(p)\frac{32\pi^2 N_\alpha p^6 e_\alpha^2}{5m_\alpha^5\gamma_\alpha c^6}\right) dp\right]^{-1/2}$$

$$A_{\max} = \left[-2D^2 \sum_\alpha \int_0^\infty \hat{F}_{\alpha 4}(p)\frac{16\pi^2 N_\alpha p^4 e_\alpha^4}{3m_\alpha^5\gamma_\alpha c^8} dp\right]^{-1/2}$$

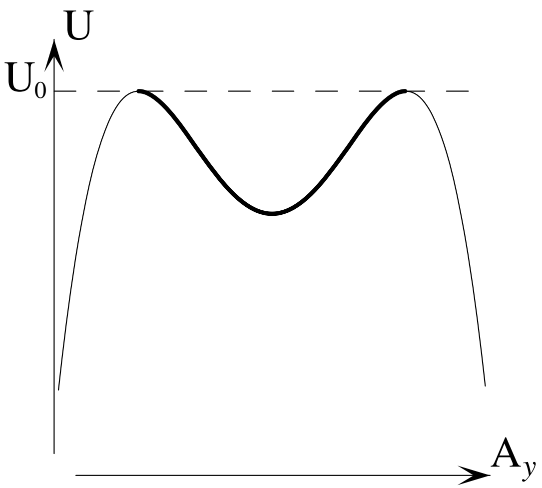

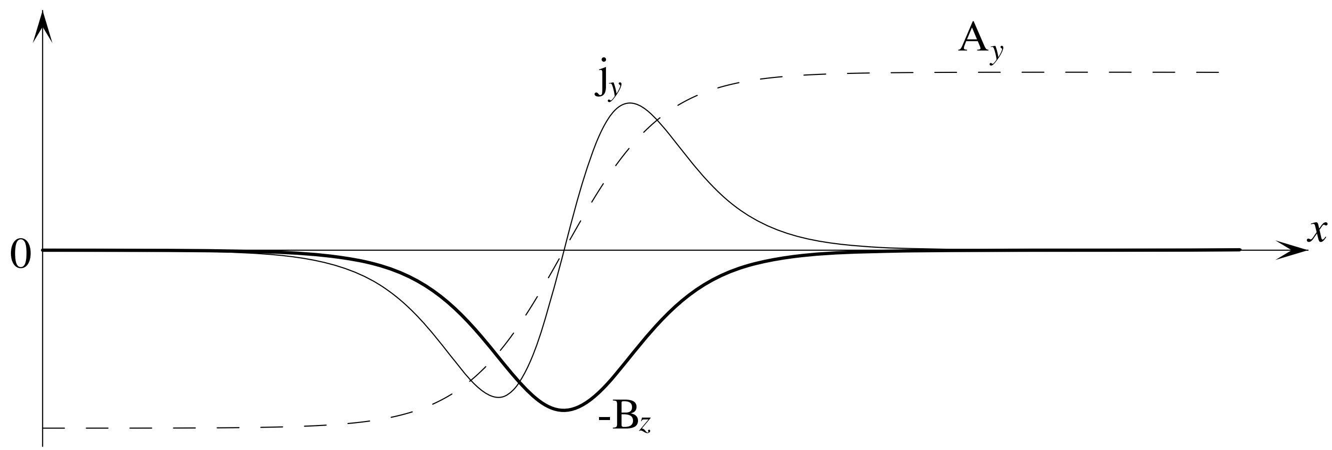

Periodic sheets (d=4)

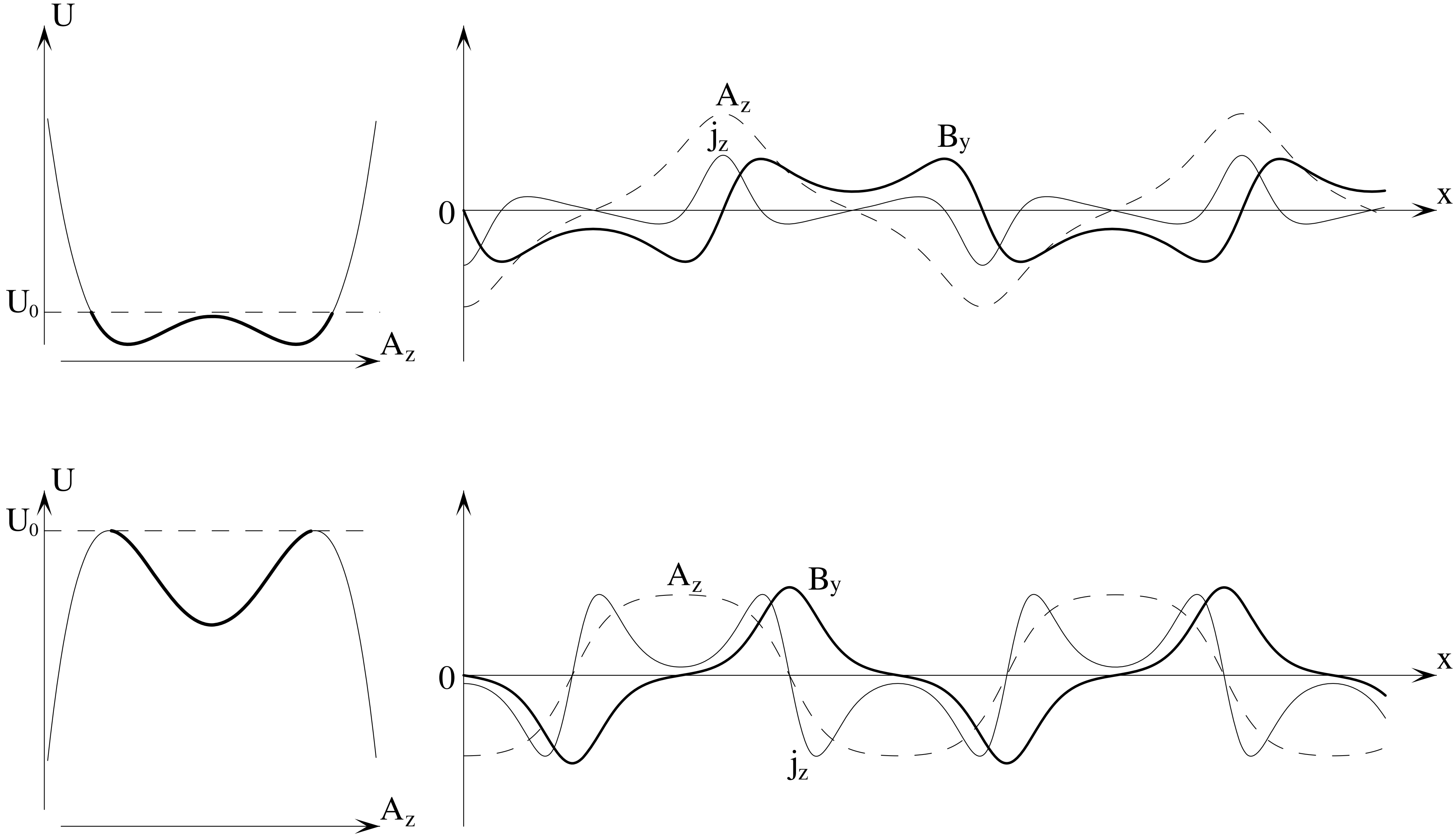

Current sheets in external magnetic field

as a boundary layer separating plasmas with different parameters

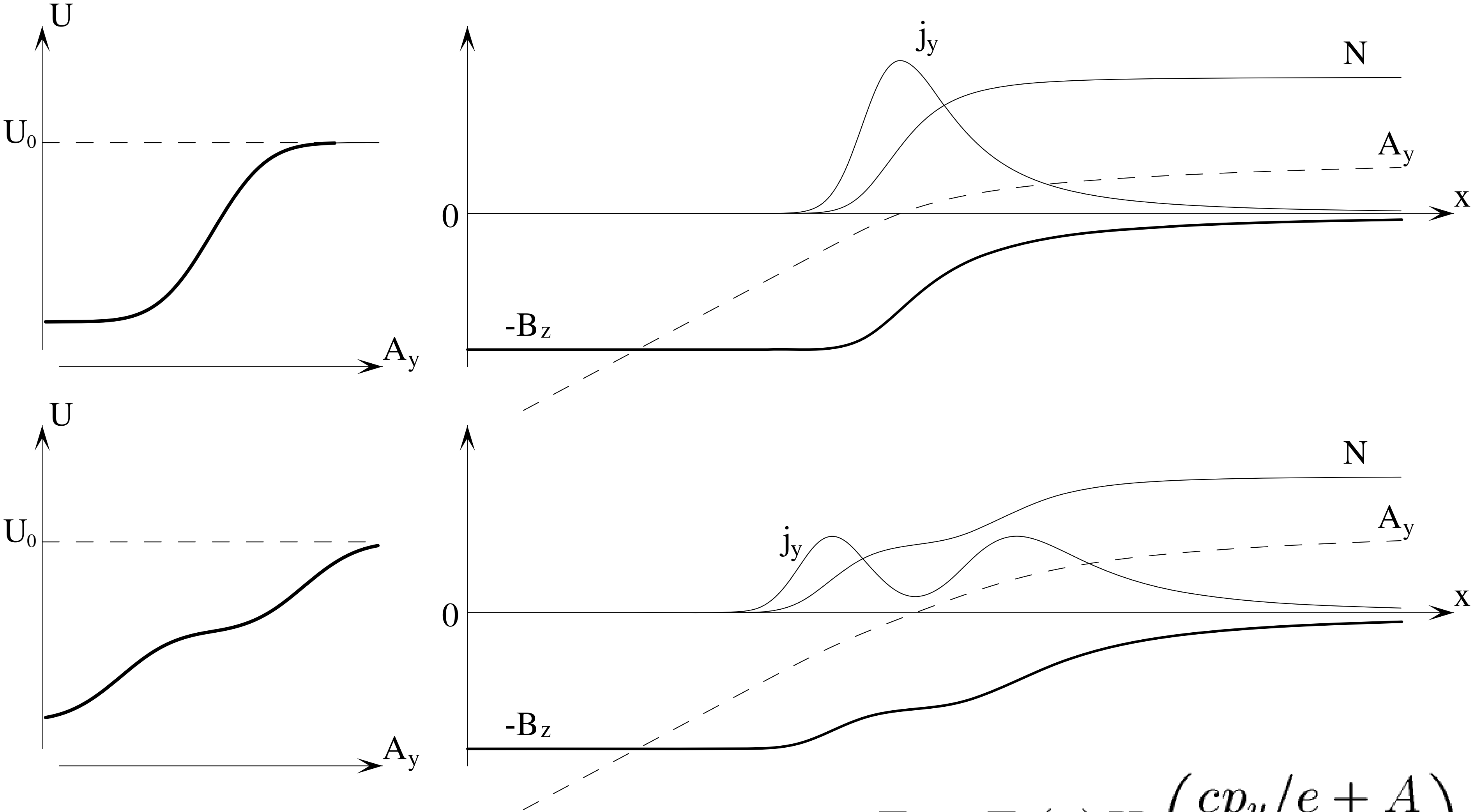

$$F = F_0(p) H \left(\frac{c p_y / e + A}{A_0} \right)$$

Boundary current sheet

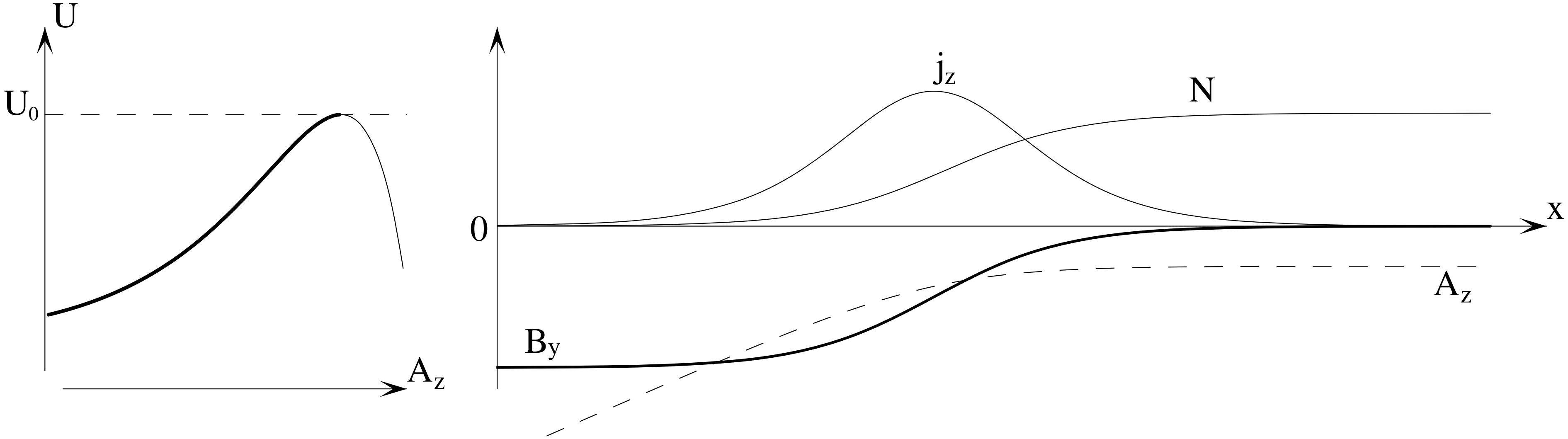

Current profile is similar to the Harris one, but PDF is different.

Boundary current sheets with step-functions in PDF

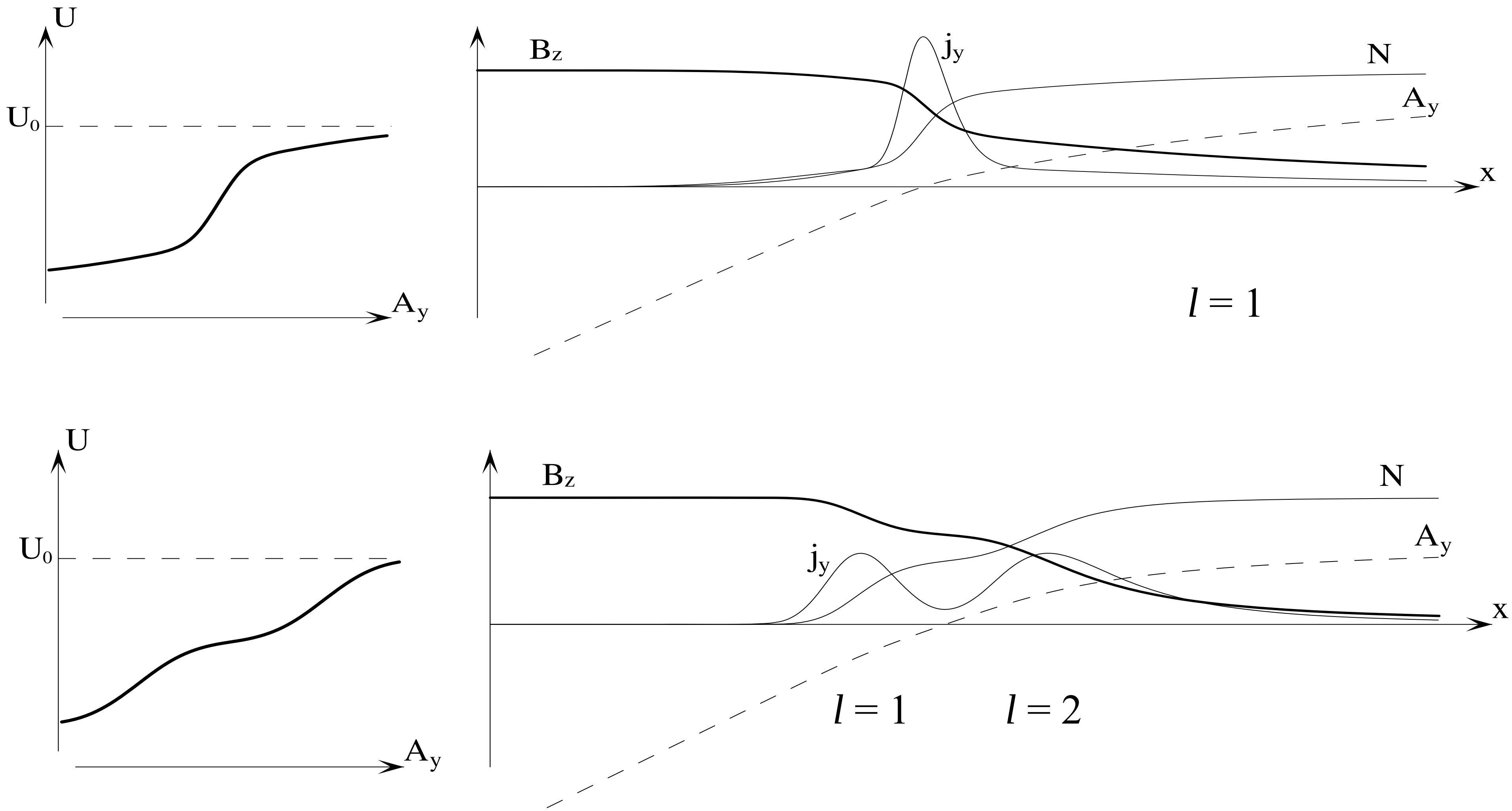

Plasma is isotropic in the regions with homogeneous magnetic field

1D current sheets with sheared chaotic magnetic fields

$$\frac{d^2 A_{y,z}}{dx^2} + \beta_1 A_{y,z} + \beta_3 A_{y,z} A_{z,y}^2 = 0$$

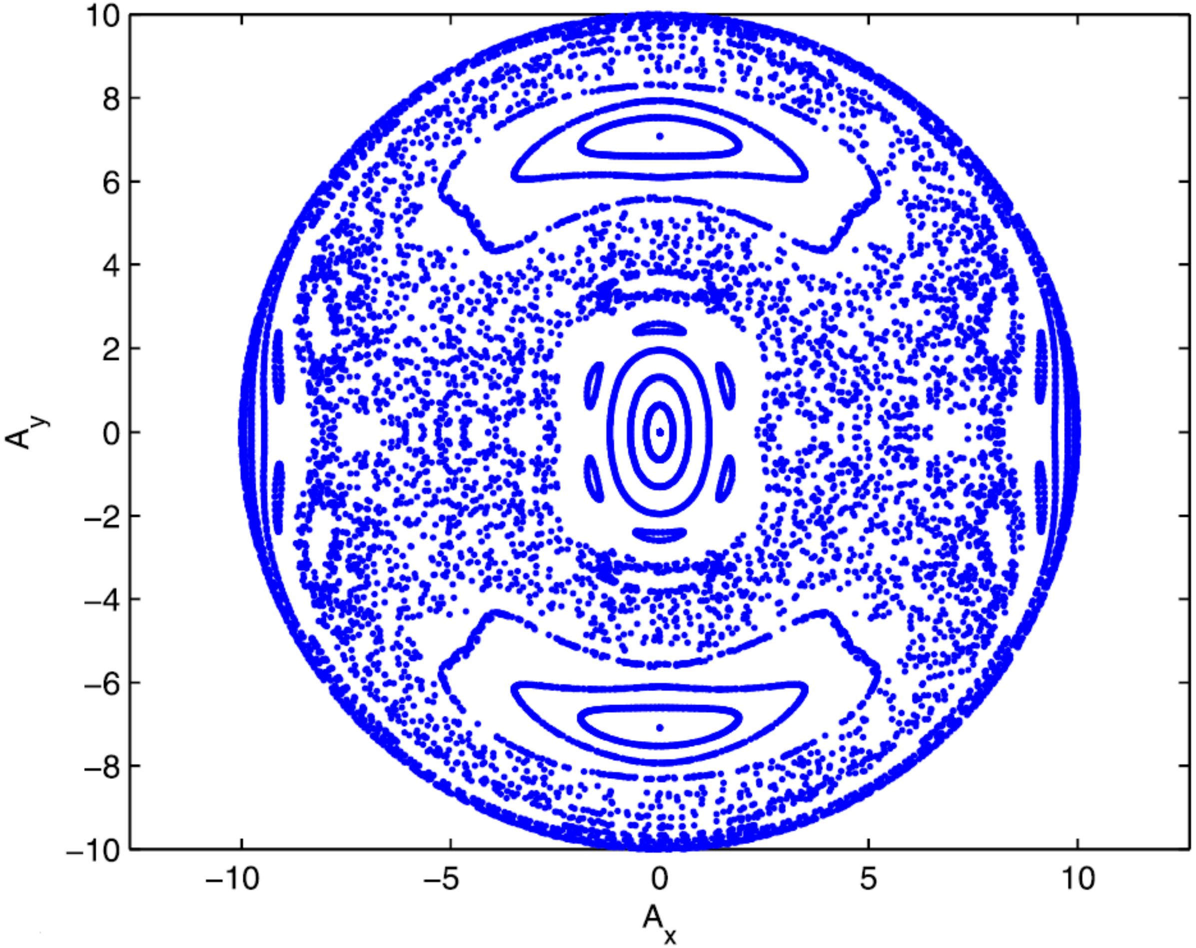

Surface of section plots in the A_x–A_y plane at B_y=0 with parameter $(r_H / L)^2 = 20$, and energy $E = 50$. [Ghosh et al. (2014)]

Cylindrical configurations (current filaments)

$$\Delta_{xz}A + k^2 A = 0; \quad k^2 = \sum_j \frac{32\pi^2 e_j^2}{3m_j^3 c^4} \int p^4 \hat{F}_{j2}(p) \frac{dp}{\gamma_j}$$

d = 2: Bessel function

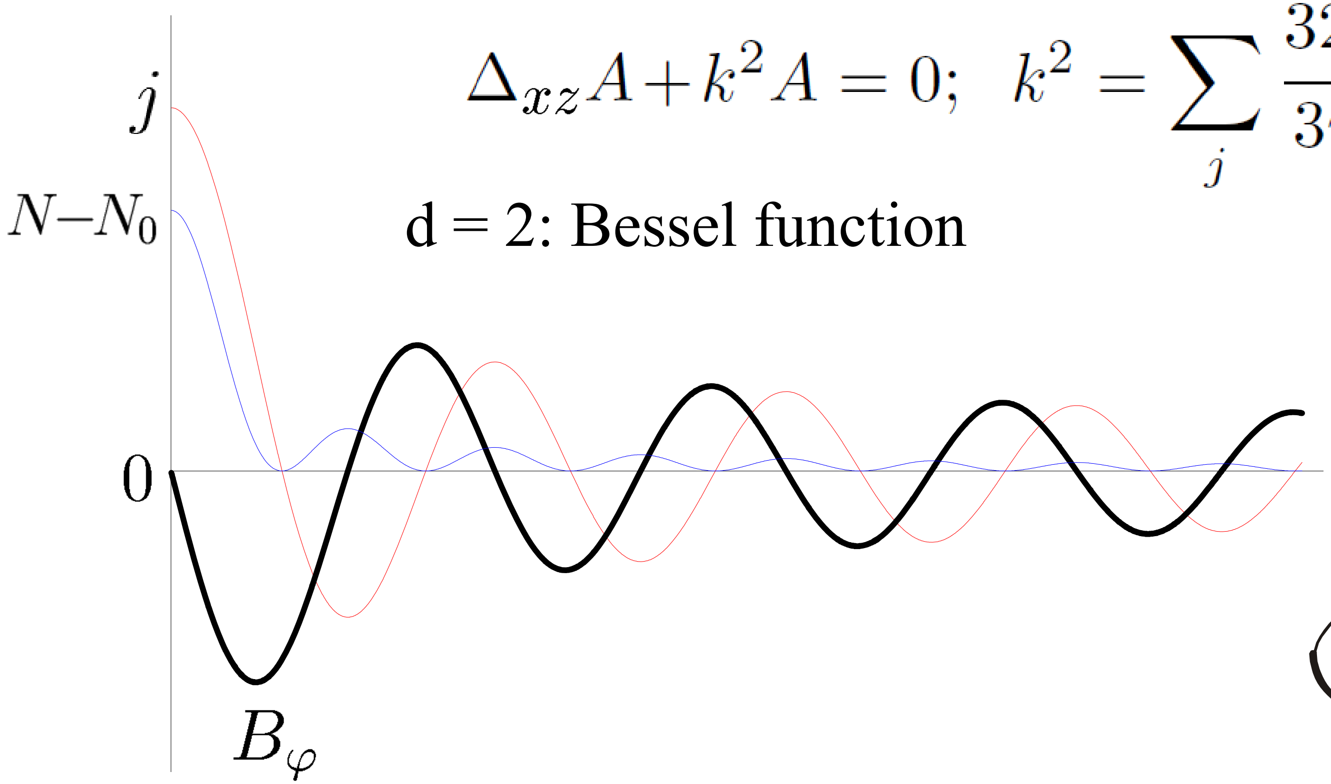

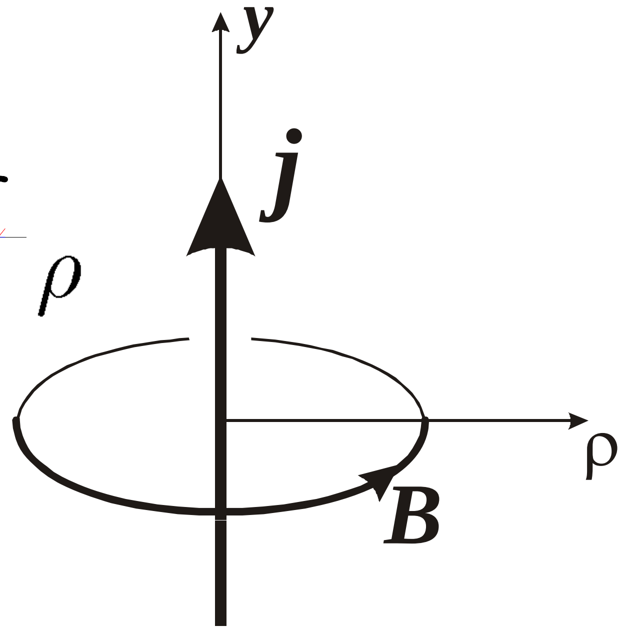

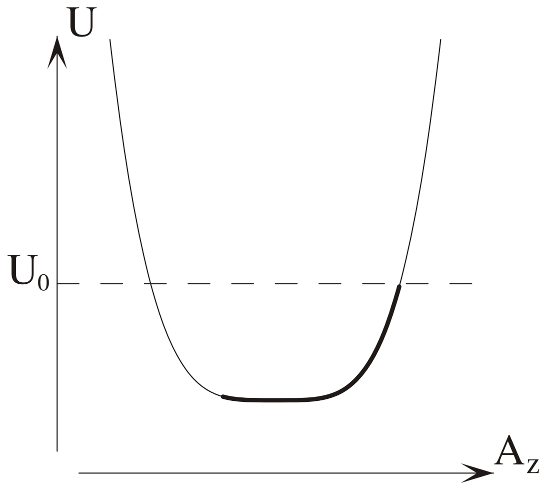

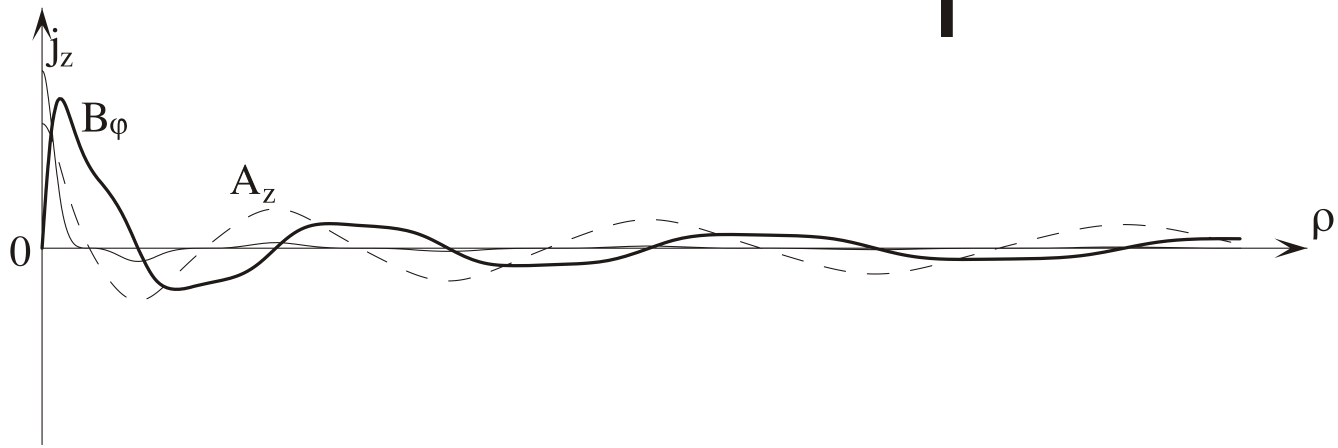

Cylindrically symmetric solutions (effective viscous damping)

$$\frac{\partial^2 A}{\partial \rho^2} + \frac{1}{\rho}\frac{\partial A}{\partial \rho} = -\frac{\partial U}{\partial A}$$

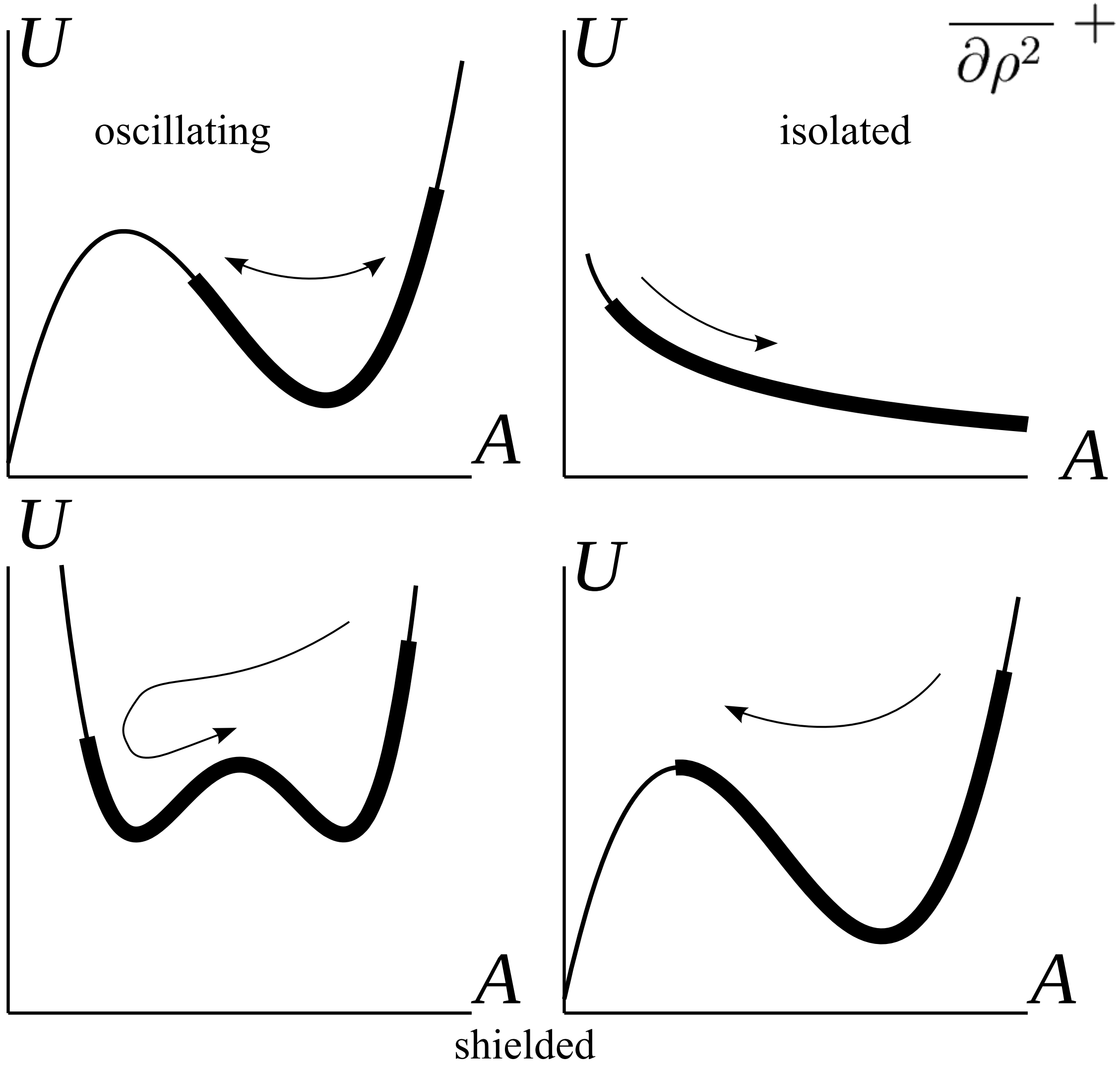

Bennett pinch (PDF of exponential type)

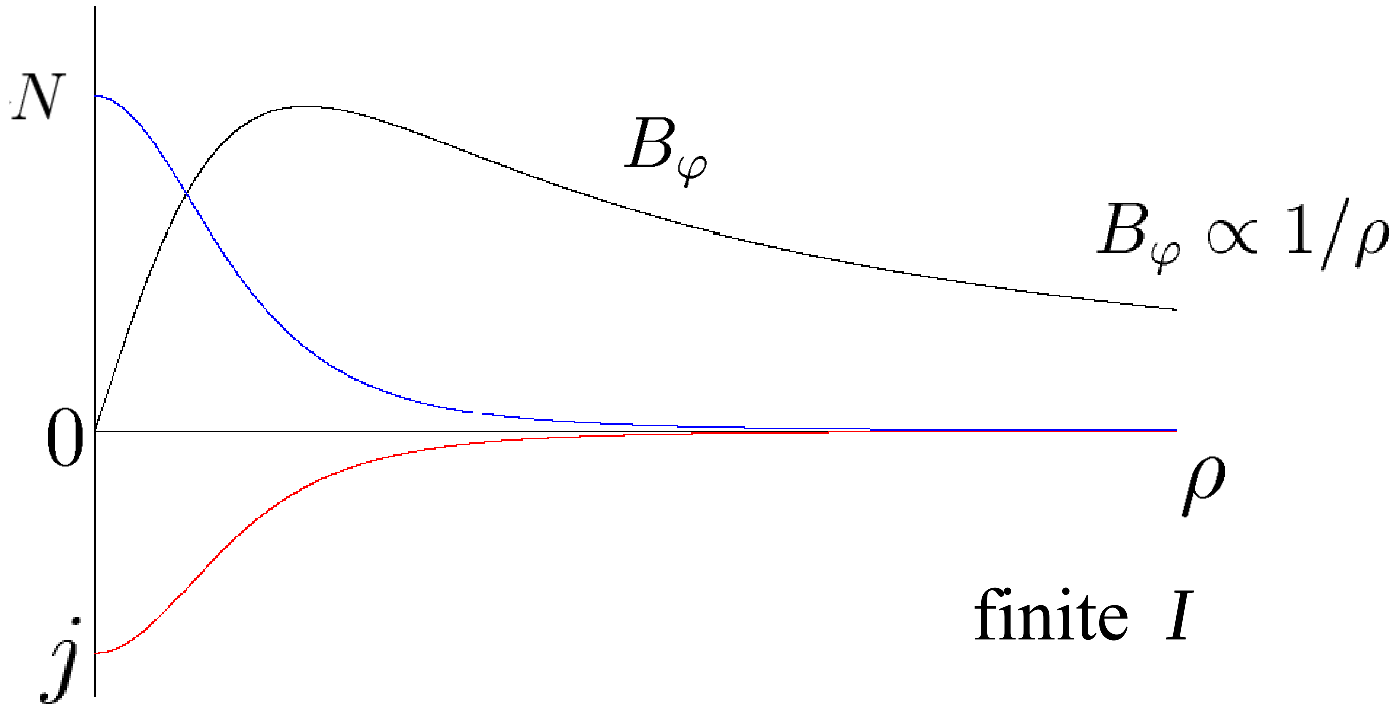

$$A = -2A_0 \ln\left[1 + \frac{\alpha(x^2+y^2)}{8A_0}\right], \quad B = \frac{4A_0\alpha\rho}{8A_0 + \alpha\rho^2}, \quad N_j = N_{j\max}\left[1 + \frac{\alpha(x^2+y^2)}{8A_0}\right]^{-2}$$

Generalized relativistic Bennett pinch

$$\frac{d^2A_y}{d\rho^2} + \frac{1}{\rho}\frac{dA_y}{d\rho} = -\frac{W_1}{A_0}\exp\left(\frac{A_y}{A_0}\right) - \frac{W_2}{wA_0}\exp\left(\frac{A_y}{wA_0}\right)$$

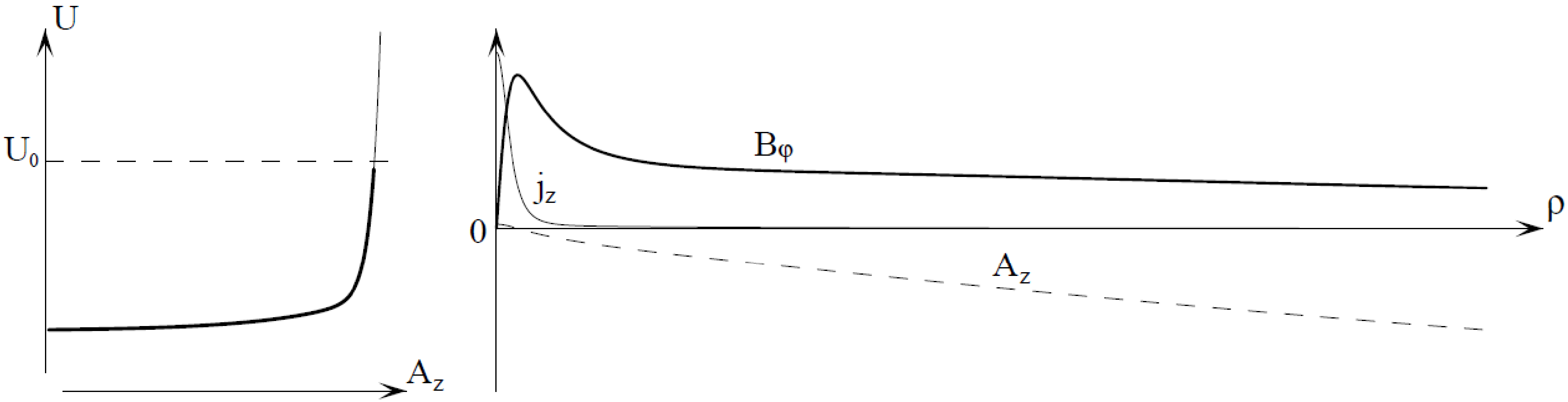

Limiting case of Bennett pinch with current along a wire on the axis $I = (1-q)cA_0$. If $q > 1$, the latter is opposite to the pinch current, which is expelled from the axis area and localized in a hollow tube.

$$B_\varphi = \frac{2A_0\left(1 - q + (1+q)(\kappa\rho)^{2q}\right)}{\rho(1 + (\kappa\rho)^{2q})}$$

$$j_z = \frac{2cA_0 q^2\kappa^2}{\pi((\kappa\rho)^{1-q} + (\kappa\rho)^{1+q})^2}$$

Shielded current filaments (Taylor order d=3, d=4)

$$I = 0$$

$$B_\varphi \propto \exp(-\rho/L)$$

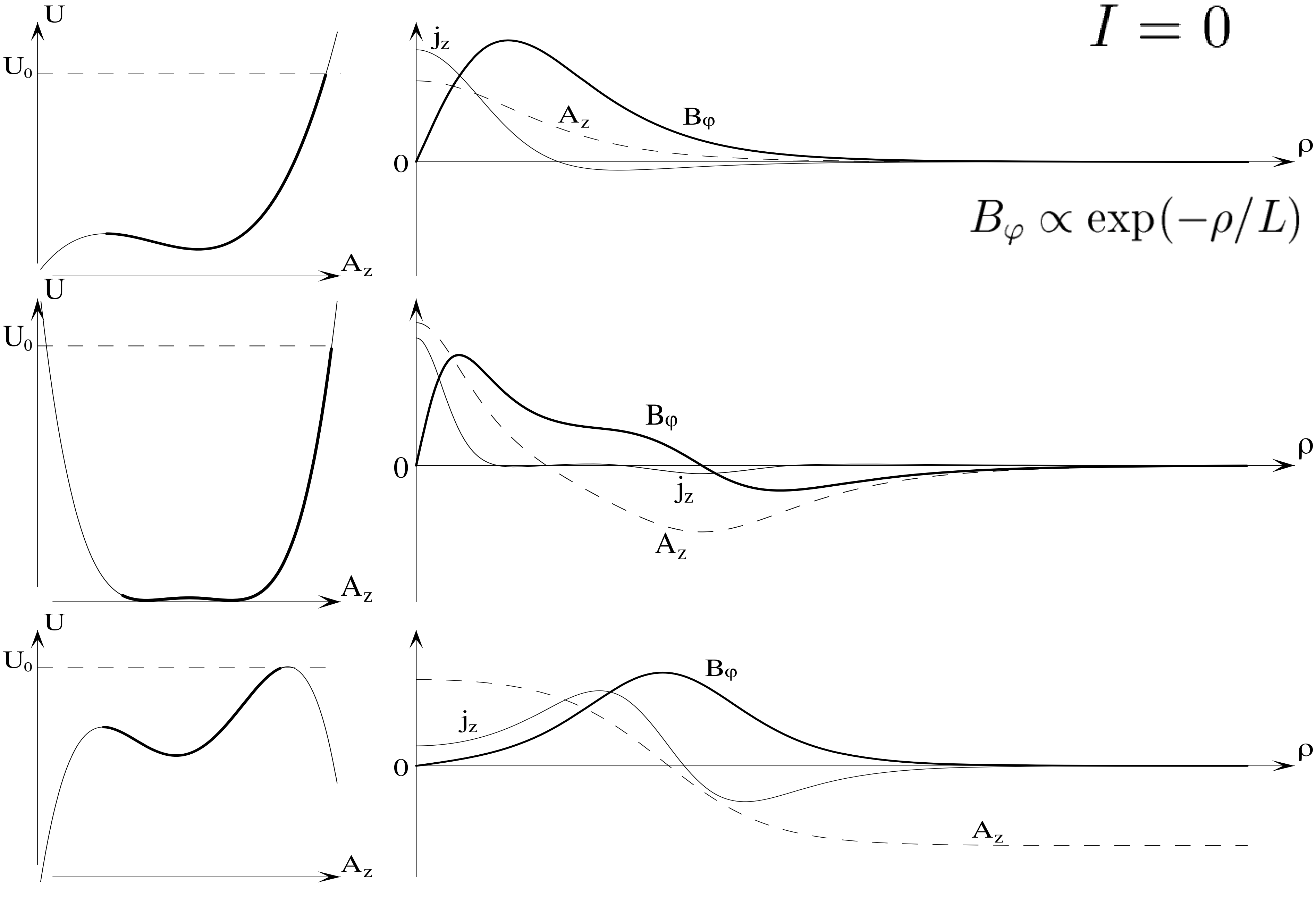

Two-dimensional current structures *j(x,z)* (*d*=2)

$$A = \sum_l A_l \cos(k\ z \cos\theta_l + k\ y \sin\theta_l + \varphi_l)$$

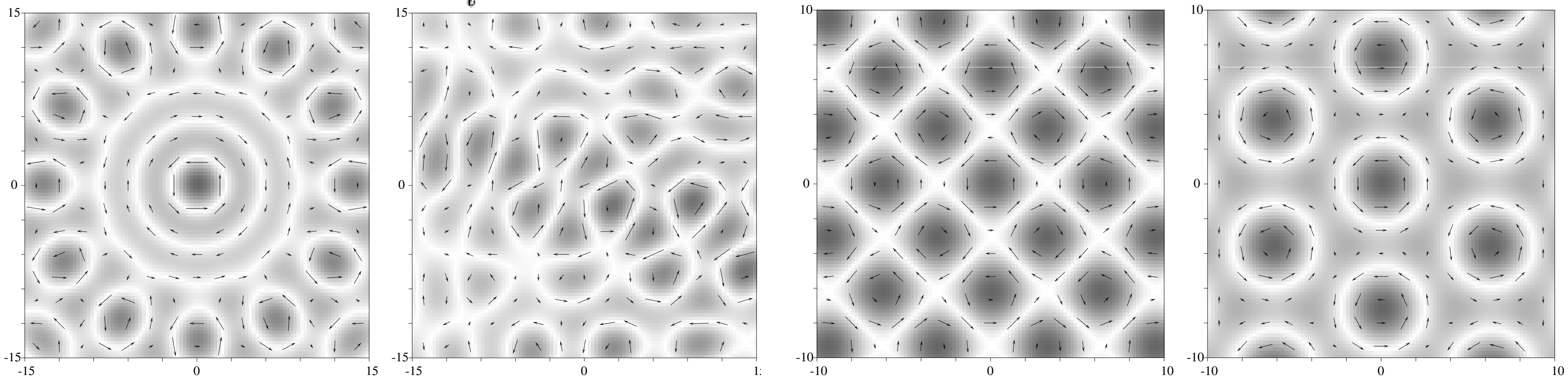

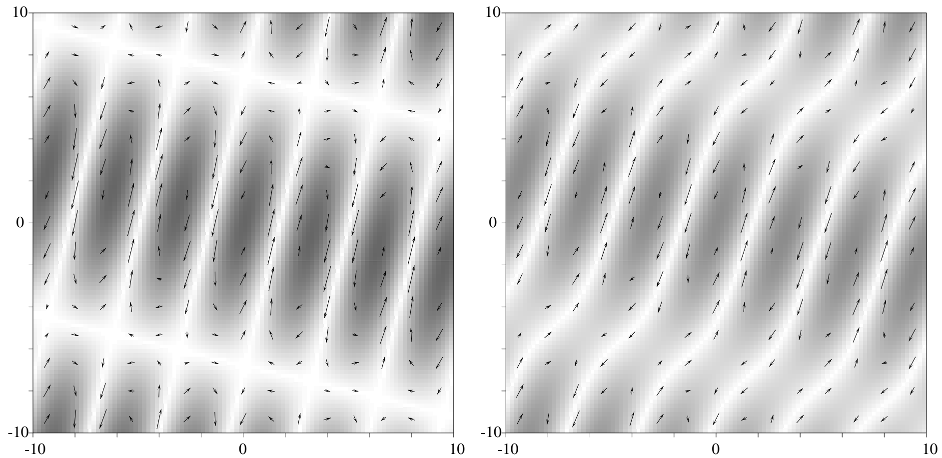

2D analytical models

$F \sim (A/A_0)^2$, $\exp(A/A_0)$, $(1+A/A_0)^{-k-1}$:

- Walker, 1915
- Fadeev, 1965
- Kan, 1973
- Manankova, 2000
- Brittnacher, 2002
- Suzuki, 2008
- Vasko, 2013

Two-dimensional Fadeev-like solution (exponential PDF)

$$A = -2A_0 \ln\left[\mu \cos\sqrt{\frac{\alpha}{2A_0}}\, \boldsymbol{z} + \sqrt{1+\mu^2}\cosh\sqrt{\frac{\alpha}{2A_0}}\, x\right]$$

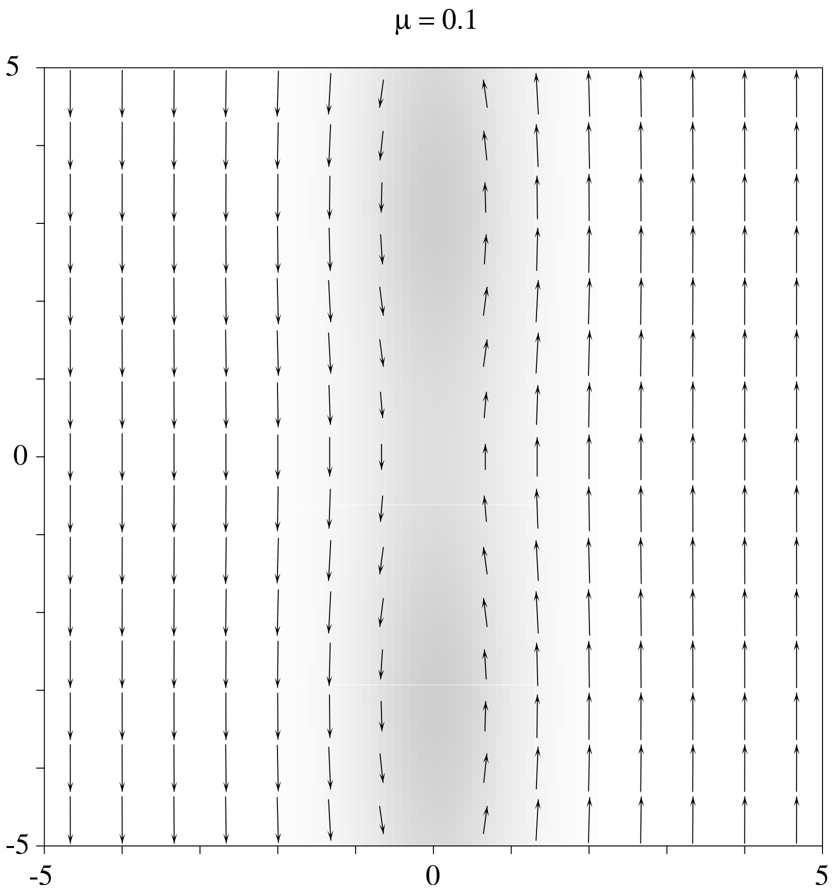

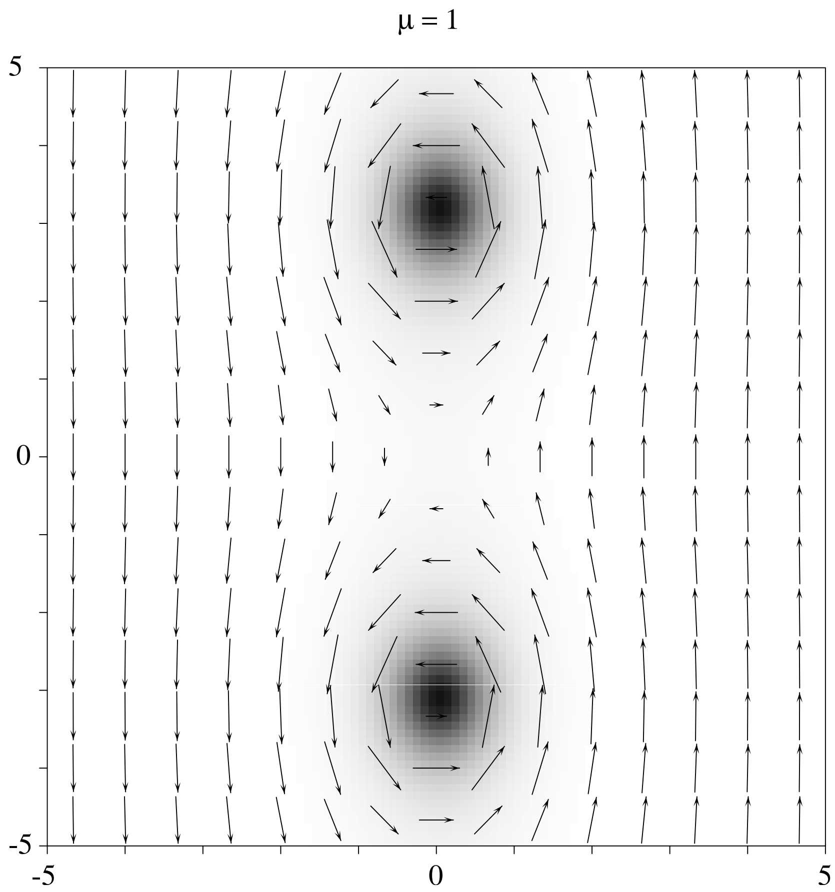

Kinetic features of self-consistent current structures

- L << r_H - most of the particles are not magnetically trapped ($I << I_A$)
- L >> r_H - the current is formed mainly by trapped particles ($I >> I_A$)

Degree of anisotropy is bounded by Taylor order *d*: $\frac{\langle p_y^2 \rangle}{\langle p_\perp^2 \rangle} < d$

Stability in the region where magnetic field vanishes:

Perturbations with ***E*** $\perp$ ***y***, ***k*** || ***y*** can be unstable for high enough $\frac{\langle p_\perp^2 \rangle}{\langle p_y^2 \rangle}$

For d=4 perturbations with ***E*** $\perp$ ***y***, ***k*** || ***y*** and with ***k*** $\perp$ ***y***, ***E*** || ***y*** are stable, if

$$\sum_\alpha \frac{e_\alpha^2}{m_\alpha} \left[5 \int \frac{f_\alpha^2(\mathcal{E})}{\gamma_a} \left(\frac{p}{mc} \right)^2 p^2 dp + 2 \int \frac{f_\alpha^4(\mathcal{E})}{\gamma_a} \left(\frac{p}{mc} \right)^4 p^2 dp \right] > 0$$

$$\sum_\alpha \frac{e_\alpha^2}{m_\alpha} \left[5 \int \frac{f_\alpha^2(\mathcal{E})}{\gamma_a} \left(\frac{p}{mc} \right)^2 p^2 dp + 6 \int \frac{f_\alpha^4(\mathcal{E})}{\gamma_a} \left(\frac{p}{mc} \right)^4 p^2 dp \right] < 0$$

Conclusions

- Closed analytical form of the nonlinear Grad-Shafranov equation is obtained on the basis of several simple decompositions of particle distribution functions (PDFs) in collisionless relativistic multicomponent plasma

- Exact solutions of magnetostatic Vlasov-Maxwell equations are found, describing a broad variety of self-consistent current filaments and sheets with arbitrary energy PDFs

- Various properties of current filaments and sheets are investigated, including magnetic energy content, gyroradius to thickness ratio, PDF anisotropy, and synchrotron radiation

- The approach presented opens the possibility to analytical modelling of current structures observed in cosmic and laboratory plasmas as well as obtained in numerical simulations

- We analyze in detail possible anisotropic features of synchrotron radiation of the self-consistent current structures and give examples of an analytical description of the breaks and the hidden components in their power-law spectra (Physics of Plasmas 22, 083303 (2015)).